Araújo, Elvis Falcão de; Guimarães, Lamartine Nogueira Frutuoso
American Space Nuclear Electric Systems

How to cite

Complete issue

More information about this article

Journal's webpage in redalyc.org

American Space Nuclear Electric Systems

Elvis Falcão de Araújo[1]; Lamartine Nogueira Frutuoso Guimarães[1]

How to cite

Araújo EF ⬤ http://orcid.org/0000-0002-6316-7073

Guimarães LNF ⬤ http://orcid.org/0000-0002-0302-9162

ABSTRACT: Since the 1960's the United States of America has launched several space missions using nuclear technology as a mean for propulsion and power supply. The majority of the American nuclear powered spacecrafts were based in radioisotope generators, with the exception of the SNAP-10A (1965), which was the only American reactor ever launched. However, some of the most notorious nuclear reactor based projects developed in the USA in the last four decades were the SPAR/SP-100 (an evolution of the Space Power Advanced Reactor program), the Space Prototype (SP-100), the Prometheus, and the Fission Surface Power (FSP). The latter is still in progress and the others were closed before its completion. This paper describes the main details about each one of these projects with the purpose of serving as a review of the technical history for the major realization steps that were conducted in the USA. This manuscript also approaches the contemporary state-of-the-art, with emphasis to the Demonstration Using Flattop Fission (DUFF) experiment and it's follow-on project, the Kilopower prototype reactor.

KEYWORDS: Nuclear energy, Fission reactors, Space missions.

INTRODUCTION

In order to stablish human development at the third millennium, it is necessary for mankind to overcome planetary restrictions and be able to explore and civilize extraterrestrial locations, which can only be done with availability of compact energy sources for power and propulsion.

There are three possible power sources that can be used for space applications: chemical, solar and nuclear (Fig. 1).

The chemical option provides high power for short periods and solar power extraction level is relatively low and depend on collector distance from the Sun and orientation, while the nuclear option takes place as an alternative option with a lot of advantages over the others, like compact size, low mass, long operating lifetime, resistance to hostile environments and high system reliability. As shown in Fig. 1, fission nuclear reactors combine higher power level and long-term operation. For missions in terrestrial orbits that require 40 kWe electrical power or higher and for interplanetary missions (power level above 20 kWe), nuclear reactors offer the best solution of electricity generation (Borges and Sielaea 1992). Radioisotope sources are long-lasting but, even for low power applications, this option is subject to the limited supply availability of ^{238}Pu.

The exploration of nuclear power consists of the usage of thermal energy that comes from exothermal nuclear reactions. Radioisotope decay and nuclear fission are the most common mechanisms. This energy can be converted into electricity by conversion devices (thermal machines or thermoelectric converters) or can be used in the direct thermal form for propulsion.
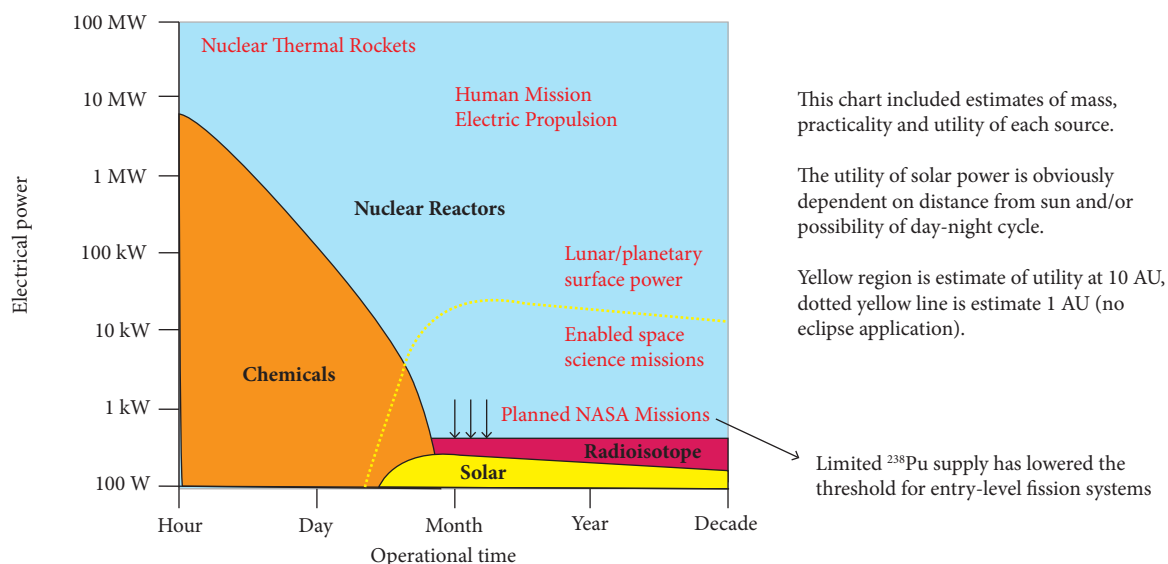
Figure 1. Time and power applicability regimes for various space power sources (McClure and Poston 2013).

Nuclear energy has been applied for spacecraft power supply since the start of the space age and its use was motivated by the Cold War. American nuclear space systems are dated from 1961, and almost all of them used radioisotope generators. The only exception was the SNAP 10-A (1965), which used uranium (^{235}U) nuclear fission. However, Russia has launched several nuclear reactors into space since the beginning of the space age. The purpose of this paper is to serve as a review of the technical history for the major realization steps that were conducted in the USA. The information contained in this review can be used as a database for future space nuclear projects. In this context, this work is intended to support the development of the TERRA (an acronym for Technology of Advanced Fast Reactors, in Portuguese) project, a Brazilian Air Force strategic project. Its concept is based on a fast-spectrum nuclear reactor coupled to a Closed Brayton Cycle by liquid metal heat pipes. This project draws inspiration from all the systems described in this review. Its design is currently under development by the Institute for Advanced Studies, located in São José dos Campos, São Paulo, Brazil. The TERRA documentation can be found in Longhini *et al.* (2017), Placco *et al.* (2017), Slewinski *et al.* (2017), Romano and Ribeiro (2017), Guimarães *et al.* (2017) and Araújo *et al.* (2017).

Although SNAP 10-A was the only nuclear reactor ever launched by the USA, some space missions using nuclear fission energy were developed in the USA throughout the years, either in nuclear thermal propulsion (NTP) or nuclear electric propulsion (NEP). Some examples are: the Nuclear Engine for Rocket Vehicle Application – NERVA/Rover (1955) in NTP; and the 710 program (1962), SPAR/SP-100 (1979), SP-100 (1983), Prometheus (2003), and FSP (2006) in NEP. The following sections will describe the most important NEP based USA's nuclear reactor space missions developed since the 1980s.

SPAR/SP-100 (1979)

PROJECT HISTORY

The SPAR/SP-100 project was an evolution of the Space Power Advanced Reactor (SPAR) program launched in 1979. It was proposed by NASA and by the Department of Energy (DOE) with the intention of creating a new generation of reactors to accommodate anticipated order-of-magnitude increases in space power needs. In 1983, the project developers felt the need of changing some elements of the SPAR/SP-100 design in order to achieve project power output and lifetime requirements. This determined the transition from SPAR/SP-100 to SP-100. This paper uses the nomenclature SPAR/SP-100 to distinguish these two projects.

The SPAR/SP-100 project was a case-of-study and none of its components were built or tested indeed, being replaced by SP-100 before further development was possible.

TECHNOLOGY OVERVIEW

SPAR/SP-100 Power design requirements include the generation of 10-100 kWe for a period of 7 to 10 years, considering 20-30 kg/kW specific power. Table 1 compiles main SPAR/SP-100 performance data. The mass and size of the nuclear power plant are affected by various factors, like payload volume limits imposed by launch vehicle, other components of the spacecraft on which the power plant will be used, and any constraints imposed by the orbital transfer vehicle used to place the nuclear-powered spacecraft in its final operation orbit. Many SPAR/SP-100 design components, such as reflector, reactivity control actuators, and shielding incorporate technologies from previous space programs (Angelo Jr. and Buden 1985).

**Table 1.** SPAR/SP-100 design parameters.

Output power (kWe)	
Range	10 – 100
Nominal	100
Reactor thermal power (kWe)	
Range	20 – 1600
Reference design	1470 kWe
Design life (years)	
Design power	7 years
Reference design	10 years
Others parameters	
Specific power	36 W/kg
System mass	2770 kg

Figure 2 is an overview of the power plant design, which is consisted by thermoelectric (TE) panels that convert heat from the reactor into electricity. The power plant geometry provides a conical radiation shielding for its non-nuclear components. Heat transfer from the reactor to the TE converters is made by heat pipes. In these components, heat transfer is made via the motion of liquid lithium, which has good thermophysical properties and is compatible with heat pipe wall and wick materials. The fluid that is used inside the heat pipes is also called "working fluid". The heat pipe evaporator temperature (~1500 K) is constrained by both power conversion system limitations and fuel swelling considerations. The fuel is uranium dioxide (UO_2) because it can support this temperature and is compatible with heat pipes material. The reactor core would operate in the fast regime due to the high power level, compact size and long operation lifetime requirements, which could not be achieved in a thermal neutron spectrum. This was known by developers from previous reactor design experiences.
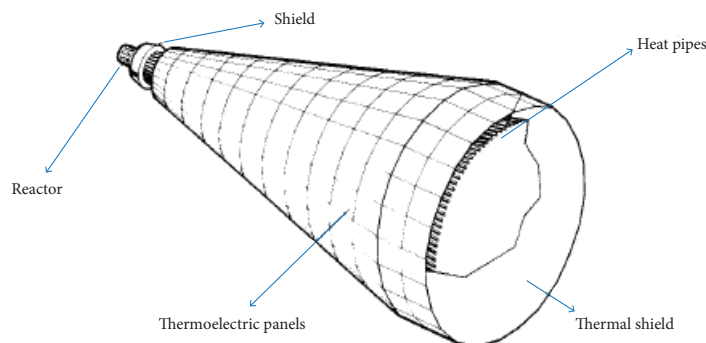
**Figure 2.** SP-100 nuclear power system (Angelo Jr. and Buden 1985).

Heat generated in reactor core is extracted by heat pipes that are radiatively coupled to the thermoelectric (TE) hot shoe thermal collectors. Heat is then conducted through TE material to the radiation panels, or the TE cold shoes, where energy that can't be used due to second law of thermo-dynamics limitations is rejected into space. TE element is depicted in Fig. 3.

Hot pipe (reactor)
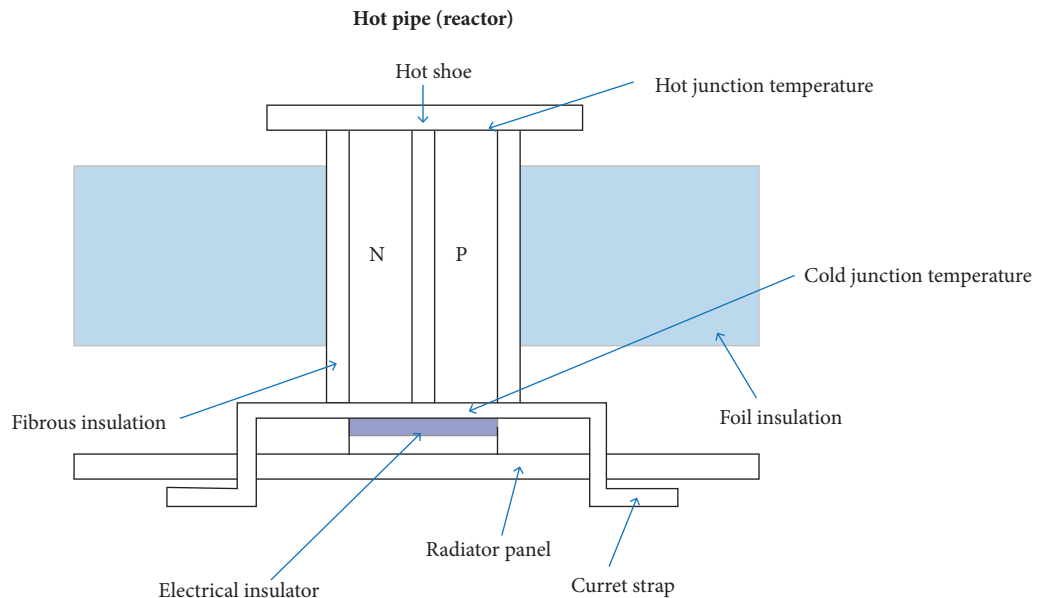
Figure 3. TE element components.

NUCLEAR SUBSYSTEM

The nuclear subsystem is responsible for heat generation and transport, and is composed basically of the nuclear reactor, the core heat pipes (HPs), the reflector (blocks radiation that can possibly escape the reactor, making neutrons scatter back to fueled region), shield (attenuates radiation levels at payload), and control system (criticality control). A schematic of this system is shown in Fig. 4.
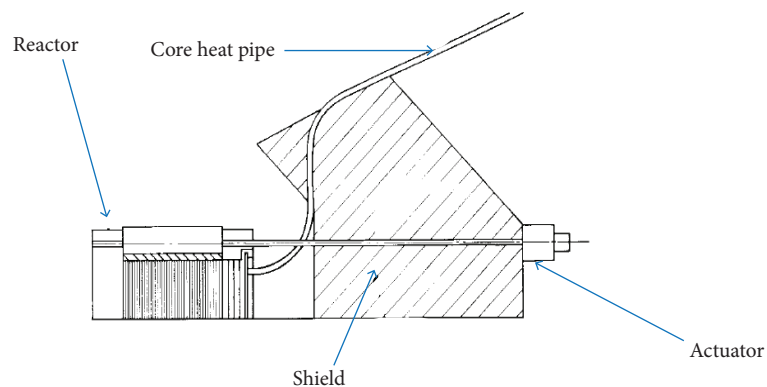
Figure 4. Nuclear subsystem schematic (Angelo Jr. and Buden 1985).

The nuclear reactor core fuel is arranged in layers between circumferential fins that are attached to heat pipes, forming the fuel modules. This feature enhances heat transfer properties and lowers the operating temperature in the UO_2 fuel, attenuating fuel swelling. The fuel module is depicted in Fig. 5. In the reactor core, these modules are disposed in concentric rings. The portions of the heat pipes within the core have Mo-13%Re (an alloy of molybdenum and 13% of rhenium) circumferential fins. Fuel tiles

are positioned in between these fins. The fuel itself is highly enriched uranium-235 (HEU) in the form of uranium dioxide (UO_2). This arrangement is surrounded by a barrel that supports the fuel modules and provides a multi-foil insulation (multiple reflective layers responsible for heat loss attenuation).
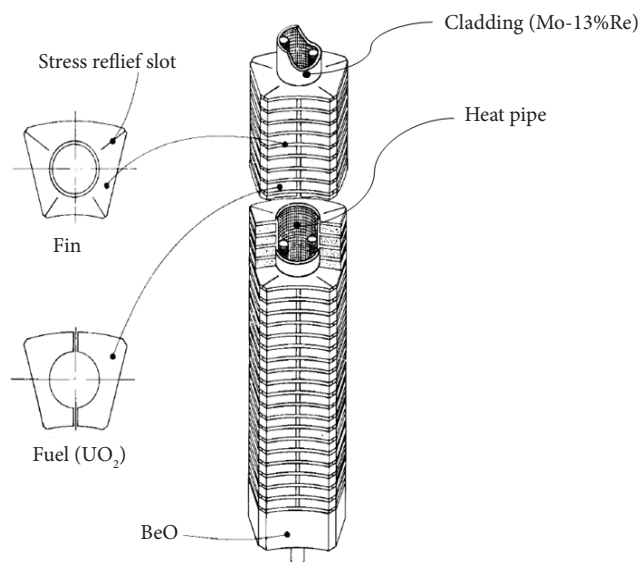
Figure 5. Typical SPAR/SP-100 fuel module (Angelo Jr. and Buden 1985).

The reflectors surround the core and are made of beryllium (Be) with parts in contact with the heat pipes being made of beryllium oxide (BeO). It operates at 800 K and is cooled by radiation from its outer surface. A special concern of this feature is the swelling caused by helium formation in (n,α) reactions, which reduces beryllium's thermal conductivity at high neutron fluences (greater than 10^{21} n/m²) and elevated temperatures (above 825 K).

The control system is composed by twelve B_4C (boron carbide) control drums disposed in a redundant configuration that avoids one-point failures in reactivity control. B_4C is a neutron absorber element that decreases criticality if inserted into the reactor core. The control drums, also called poison plugs, are located within the reflectors and are rotated by electro-mechanical actuators. Reactivity is increased or decreased by moving the reflector absorbing material away from or towards the core, respectively. Therefore, control drums are responsible for flattening of k-eff during reactor operation. The actuators are located away from the core behind the shield (see Fig. 4) for protection against both nuclear and thermal radiation. There is also a void space in the center of the core that accommodates a B_4C poison plug. This is a safety feature to keep reactor subcritical even if the heat pipes fail. Once the reactor and its spacecraft are on orbit, this plug is removed. Figure 6 is a drawing of the fully mounted reactor.

The radiation shield is located between the reactor and the payload. Its design is based on the shielding of the SNAP program. It is composed of lithium hydride (LiH) for neutron protection and a layer of tungsten (W) for gamma radiation shielding.

The shield operating temperature is at least 600 K to permit reabsorption of radiolytically decomposed hydrogen, preventing swelling. Also, it must remain below 675 K to avoid hydrogen loss due to excessive thermal dissociation if spacecraft casing is damaged.

There are distinct axial and radial power profiles in the core, but a uniform amount of heat generation per module is predicted. Criticality is achieved by using a specific mass of HEU inside the fuel modules. In normal operation, all the core heat pipes should transport about the same amount of thermal energy.

The heat pipes come from the reactor core, bend along the radiation shield and go to the TE system, as shown in Fig. 4. Heat pipe and core cladding material is Mo-13%Re, which is compatible with the working fluid and fuel and also has good high temperature creep strength and good ductility below 200 K. The same material is used in reactor vessel.
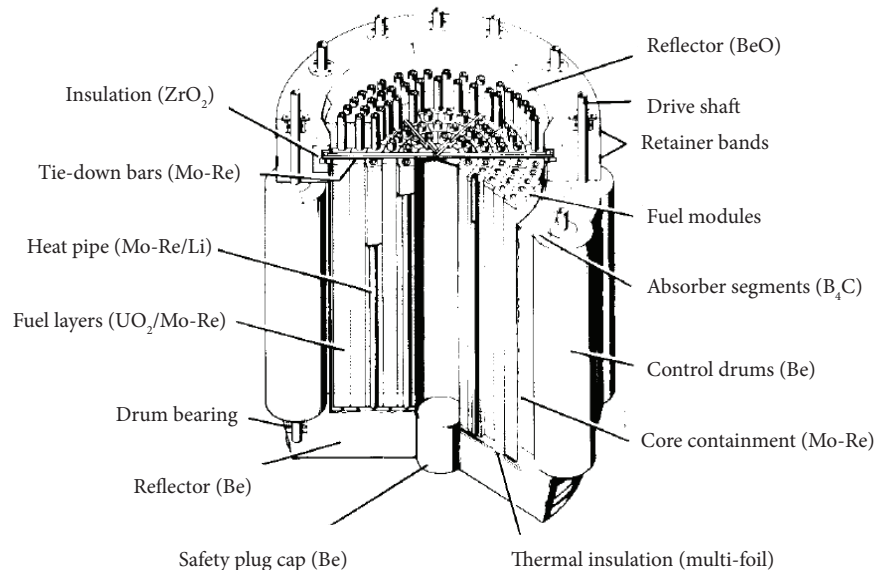
Figure 6. SPAR/SP-100 reactor core section view (Angelo Jr. and Buden 1985).

A heat pipe artery wick design provides low-pressure drops and avoids single point failures. The circumferential distributive wick transports the condensing fluid to and from the arteries, while the arteries transport lithium axially. A section view of the heat pipe with the wick configuration is represented in Fig. 7. The evaporator sections of the heat pipes are located inside the reactor core and the condenser sections are coupled to the TE converters, which eliminates the necessity of pumps to conduct lithium flow, as fluid goes one way by pressure gradient and comes back by capillarity. After launch, the lithium is naturally thawed out as it reaches the operating temperature. Heat transfer from the core to the heat pipes is responsible for raising lithium temperature. System power and lithium flow rate are limited by heat pipe performance limitations. In this particular design, these restrictions are represented by the sonic limit and the capillary action that can be achieved with a given wick pore size. Figure 8 shows the predicted behavior of a core heat pipe. Table 2 compiles design data about SPAR/SP-100 nuclear subsystem (Angelo Jr. and Buden 1985). The value of lithium flow rate was calculated from the heat pipe temperature gradient, the normal operating power and the liquid Li thermophysical properties (Davison 1968).
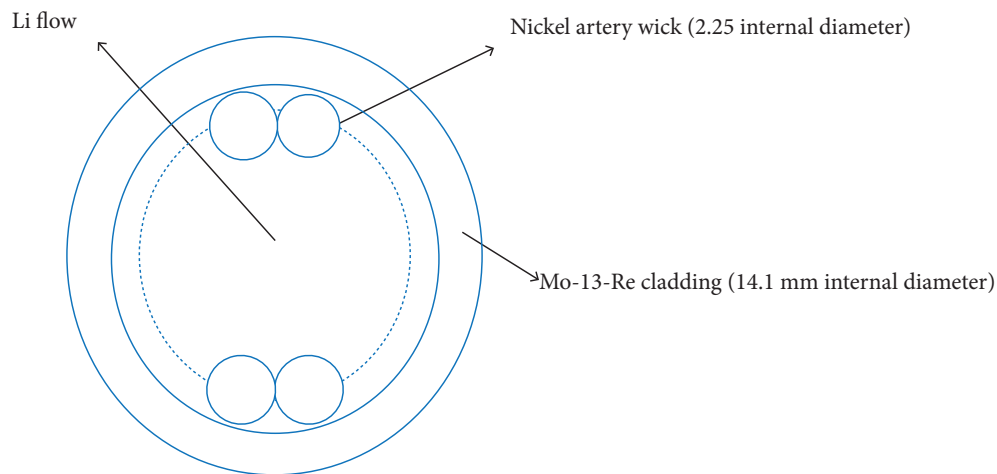
Figure 7. SPAR/SP-100 heat pipe cross section with artery wick configuration (Angelo Jr. and Buden 1985).
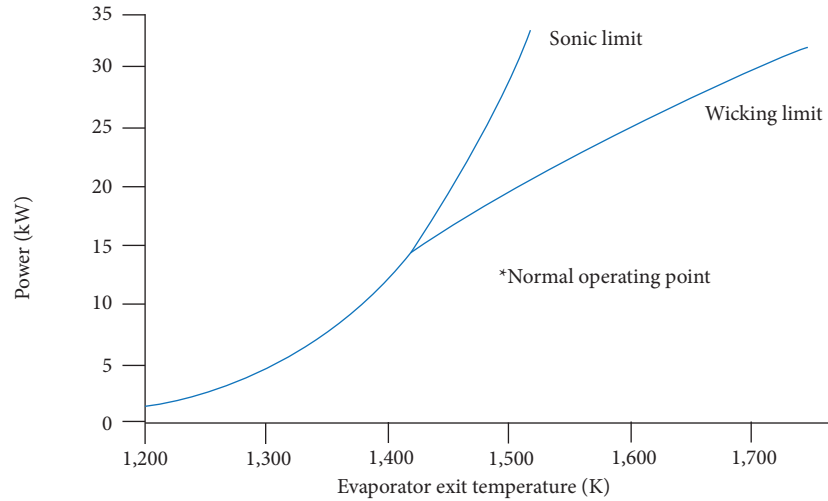
Figure 8. Typical high temperature heat pipe performance curve (Angelo Jr. and Buden 1985).

Table 2. SPAR/SP-100 nuclear parameters.

Parameter	Value
Thermal power (MW)	1.5
HP evaporator temperature (K)	1500
Number of HPs (–)	120
Number of fuel modules (–)	120
HP materials	Contrainer: Mo-Re
	Working fluid: Li
Single HP nominal power (kW)	~ 13.75
Single HP mass flow rate (kg/s)	~ 0.023
Max UO_2 temperature (K)	1730
Nuclear subsystem mass (kg)	440
Beginning-of-life reactivity (–)	1.05
Core diameter (cm)	33
Core height (cm)	33

POWER CONVERSION

The SPAR/SP-100 Power Conversion subsystem is consisted of TE converters, thermal insulation to isolate radiators from nuclear core heat source, interconnecting circuitry between TE converters and power processing equipment, and coating materials to protect TE material from high temperature sublimation. The cold shoes of the TE converters are the power plant's radiators, being responsible for waste heat rejection.

Conversion efficiency depends on chosen TE material. By the time the reactor was being developed, the most common material for TE conversion was Silicon-Germanium (SiGe). However, boron carbides and rare earth compounds were found to be the most desirable materials for its long-term stability in high temperatures, good strength capacities, and facility to be bonded to other materials. The major concern was the sublimation limitation, which could be reduced by proper coating. The TE converters are disposed in panels that are assembled together forming a frustum of a cone (see Fig. 2). Thermal energy is conducted by radiation transfer from the heat pipes to the TE hot shoes, whose material need to have compatibility with the thermocouples, light weight, good thermal conductivity, and capacity of operating at 1355 K.

Compounds of molybdenum (Mo) and carbon (C) were good candidates. Multifoil insulation is used for thermal isolation between the hot and cold shoes. Table 3 shows the main design parameters of the SPAR/SP-100 power conversion subsystem.

Table 3. SPAR/SP-100 power conversion parameters.

Parameter	Value
Electrical power	100 kW
Efficiency	6.8 %
Hot junction temperature	1355 K
Cold junction temperature	840 K
Hot shoe material	Graphite
Cold shoe material	Carbon/Carbon composite
Radiator temperature	800 K

SP-100 (1983)

PROJECT HISTORY

In 1983, the National Aeronautics and Space Administration (NASA), the Department of Energy (DOE) and the Department of Defense (DOD) joined efforts to launch the SP-100 program, a new space nuclear program with the objective of developing a 10 year life (7 years at power) space nuclear reactor power system operating in the range of 10 to 1000 kWe for use in the future military and civilian space missions (Smith 1989).

The SP-100 space nuclear reactor was designed to be a highly flexible power supply for orbital systems, Lunar or Martian surface power stations, and nuclear electric propulsion (NEP). Originally, the project was an orbital power supply for the US Strategic Defense Initiative (SDI). Although the original sponsors were DOD, DOE and NASA, the demise of the Soviet Union reduced SDI efforts and the missions evolved more towards the needs of NASA. By the early 1990s, the grandiose missions of NASA came into question, and the priority was given to more palatable missions. Besides, funding problems required a restructuring of the program to demonstrate a full technology and lifetime test by 1998. These problems lead SP-100 to its discontinuation in 1995 (Demuth 2003).

The program was divided into three phases: Concept Selection, Technology Development/Validation, and Flight Demonstration. The first three years of program were dedicated to the first phase.

Four power conversion systems were considered: in-core thermionics, thermos-electrics, Stirling engines, and Brayton machines. The latter three concepts used a fast spectrum, lithium cooled, uranium nitride (UN) fueled nuclear reactor, while the first reactor was UO_2 fueled. The dynamic cycles represented by the third and fourth options had potentially much higher efficiency than the others, but operation vibrations could cause system failure.

Feasibility investigations were conducted by a team of DOE and NASA laboratories working with aerospace companies and associated nuclear reactor companies. All of the concepts were found to be safe and feasible, but after carefully weighting of pros and cons, the thermoelectric system was selected for development under phase II of SP-100 in 1985 (Smith 1989).

The SP-100 reference flight system (RFS) design is shown in Fig. 9. The overall weight goal of the RFS was approximately 4500 Kg such that the power system and a reasonable payload could be launched using either the Space Shuttle or the US Airforce Titan IV launch vehicle (Smith 1989). The conical geometry is a shielding feature to protect the other RFS components from nuclear radiation. This characteristic was also present in the SPAR/SP-100 system.

NUCLEAR COMPONENTS

The SP-100 nuclear reactor is depicted in Fig. 10. It is a UN fueled, lithium cooled fast reactor with nominal design for 2.5 MWt of thermal power in order to produce a minimum of 100 kWe of electricity by thermoelectric conversion, with technology scalability of 10 kWe up to 1000 kWe. It is designed to have 7 years of continuous operating lifetime.
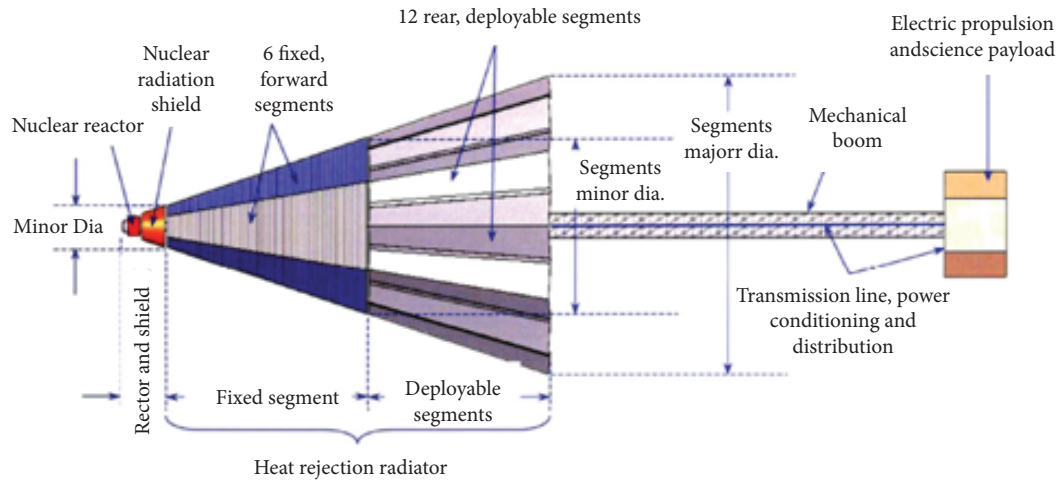
Figure 9. 100 kWe SP-100 high temperature reactor with thermoelectric power conversion concept (El-Genk 2009).
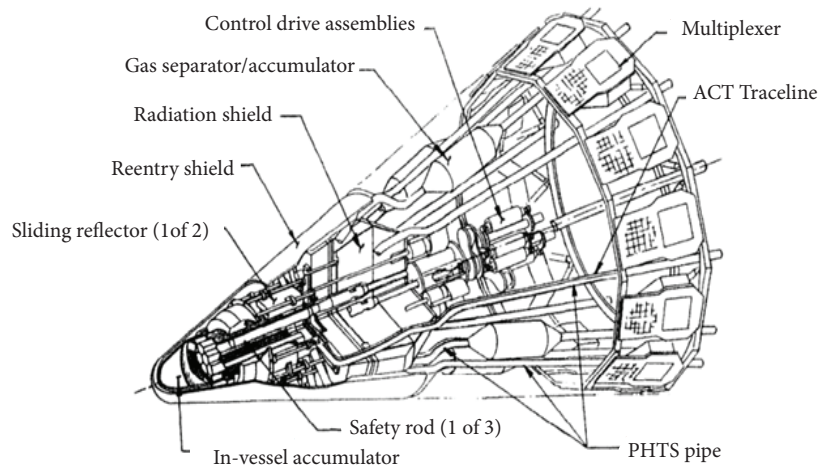
Figure 10. SP-100 reactor components (Demuth 2003)

The composition material of the reactor vessel, fuel pin cladding, and primary heat transport system components is PWC-11 (niobium, 1% zirconium, 0.1% carbon).

Three boron-carbide safety rods are inserted inside the reactor core to assure shut down conditions for all possible accident scenarios. A safety plug (made of B_4C poison, BeO reflector and W and LiH shield sections) is used to guarantee subcriticality in case of water core immersion. During launch, this plug is inserted into the core. While in orbit, the safety plug is moved such as the reflector section stays in the core.

Twelve beryllium oxide (BeO) reflector elements surrounding the reactor provide neutron scattering during startup, shutdown and power operation regimes.

The nuclear shield is composed of multiple layers employing tungsten (W) for gamma ray attenuation, lithium hydride (LiH) for neutron shielding and beryllium (Be) for thermal control and structure. A titanium shell designed to protect the RFS components from nuclear core radiation within a 17° half angle (chosen for mass minimization) cone contains the Nuclear Shield. Reactor core provides thermal energy to Li working fluid at 1375 K.

HEAT TRANSFER AND POWER CONVERSION

The heat transport system is composed of twelve heat pipe loops carrying nuclear reactor lithium coolant to the hot side of the TE converters. The coolant flow to primary loop initially passes through a Gas Separator/Accumulator (GSA) that scavenges helium bubbles generated within the reactor (Demuth 2003). This component is present into coolant flow loop to avoid helium build up by lithium neutron capture in the reactor, which can produce hot spots and over pressurization (El-Genk 2009). The secondary cooling loops remove radioactive decay heat and maintain the core temperature at a low enough level (2000 K) to insure fission products retention and structural integrity in case of an accident with coolant loss (Smith 1989).

After passing through the power conversion system, lithium coolant is pumped back to the reactor core by EM pumps. These devices also carry lithium coolant along the heat rejection loop. The EM pumps use the temperature difference between the hot primary loop and the cold heat rejection loop to drive its own thermoelectric power unit, which means they are self-sustainable (Smith 1989). Figure 11 shows a functional integration of SP-100 system in a block diagram.
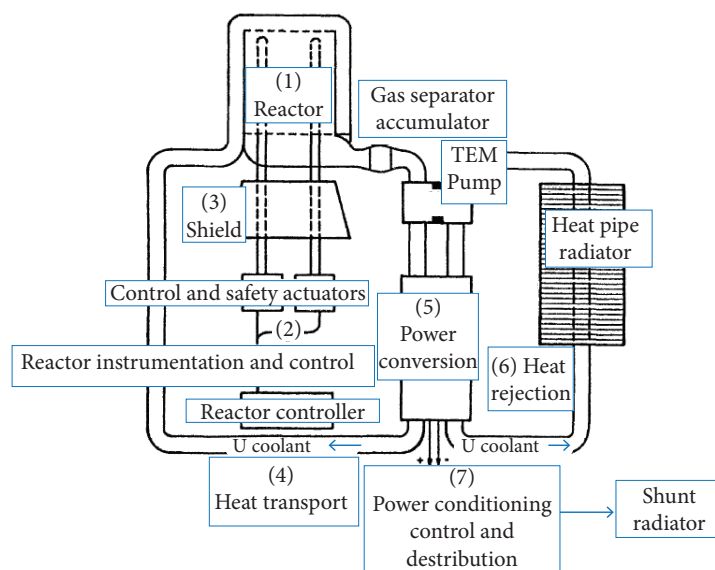
Figure 11. SP-100 functional layout (Demuth 2003).

Both main power conversion and pump thermoelectric elements are conductively coupled and made of silicon-germanium doped with gallium-phosphide (SiGe + GaP). There are 12 TE assemblies. Each TE assembly has a total of 720 cells located on six "plate and frame" assemblies each of which produces 1.5 kWe. Therefore, the SP-100 nominal power is 12 (TE assemblies) × 6 ("plate and frame" assemblies) × 1.5 (kWe/assembly) 100 kWe.

Twelve heat rejection loops composed of titanium (Ti) tubes filled with lithium cool the cold side of the thermoelectric elements and bring the waste heat to the radiator, which is composed of multiple heat pipes using potassium (Na) as working fluid (Smith 1989). The heat rejection loop operation temperature is 800 K.

PROMETHEUS (2003)

PROJECT HISTORY

The JIMO (Jupiter Icy Moons Orbiter) mission was a program launched by NASA in partnership with the Naval Reactors Contractor Team (NRPCT) to develop a 200 kWe electric reactor plant with 15-20 year mission applicable to nuclear electric propulsion (NEP).

Prometheus Project precursor studies, referred to as Jupiter Icy Moons Tour (JIMT) studies, initiated in September 2002, where three parallel studies with solar power, radioisotope thermal generation (RTG) and fission power sources were conducted. In November 2002, the NASA administrator Sean O Keefe selected nuclear fission for further pre-project study.

The JIMO project was officially initiated as a NASA project in 2003, when the Jet Propulsion Lab (JPL) established the JIMO Project Office. The level 1 requirements for JIMO were then established, stating that the project would perform a scientific exploration mission to Callisto, Ganymede and Europa, the Icy moons of Jupiter. The responsibilities for the JIMO project (now known as Prometheus) were designated on March 2004.

Prometheus was to be developed consistently with NASA life cycle for flight projects, being split into five steps: pre-phase A (advanced studies), phase A (mission and systems definition), phase B (preliminary design), phase C/D (design & build/assembly, test and launch operations), and phase E (Operations).

Technology concept selection was one of highlights of the work done in 2004. Previous feasibility studies lead to the conclusion that fuel, materials and system integration would be the major operational concerns. The candidate options were selected based on these studies. Three of them used Brayton power conversion, with the coolants being respectively a gas, heat pipes and liquid Li. The fourth used TE elements with liquid Li coolant, and the last one used a liquid Na cooled reactor with Stirling conversion (Ashcroft and Eshelman 2007). The first candidate was chosen and approved by NR headquarters after an evaluation of the overall system features, including capability, reliability, deliverability, cost and safety. Power compatibility with mission requirements, simplification of development testing, and minimization of hurdles to development were among the advantages of this concept.

Reactor physics, thermal and mechanical design evaluations, reactor core and plant arrangements, integrated system performance estimates, evaluation of material options, instrumentation and control development, and reactor plant operating scenarios were among the studies made. This was part of the Prometheus mission and systems definition, which was predicted by phase A of the project life cycle.

However, NASA re-evaluated its priorities in light of available funding. NEP based missions, like Prometheus, were given third priority, behind nuclear surface power and NTP. Consequently, Prometheus project was directed to not proceed into Phase B. In addition, it was asked to support a NASA study, called the Exploration Systems Architecture Study (ESAS), in the area of lunar surface power, delivering the Lunar Fission Surface Station Study Final Report on August 17, 2005. The Prometheus project was officially discontinued by October 2, 2005 (Ashcroft and Eshelman 2007).

TECHNOLOGY OVERVIEW

The Prometheus spaceship is consisted of three major elements: the Reactor Module, the Spacecraft Module and the Mission Module. Two parts, the Reactor Module and the Spacecraft Module, combine to form the Deep Space Vehicle (DSV), which is the basic vehicle that provides the engineering functionality to support multiple missions. Figure 12 shows an overview of the
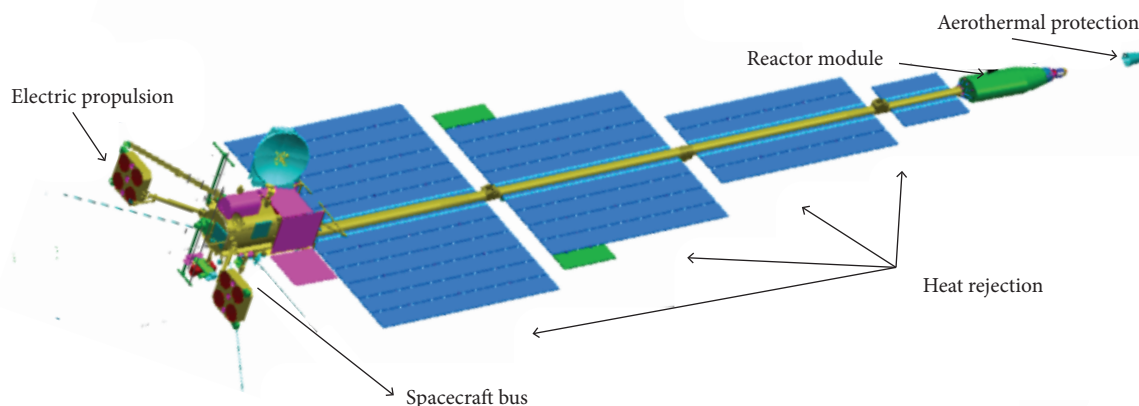
Figure 12. Prometheus DSV isometric view (Ashcroft and Eshelman 2007).

DSV, and Table 4 states main performance parameters of Prometheus pre-conceptual base case. Study of options that could be alternatively used was included in project scope (Randall 2005). The final concept was not decided until project closeout in 2005. The Mission Module is unique for each mission and it is coupled to DSV so it can perform a diverse number of missions.

Table 4. Prometheus reactor plant parameters.

Parameter	Value
Electrical power	200 kWe
Nominal core thermal power	1000 kWt
Mission duration	15 years
System efficiency	18.2%
Reactor inlet temperature	891 K
Reactor outlet temperature	1150 K
Number of braytons	4
Braytons configuration	Two 100%, Two spare
Working fluid	He-Xe mixture
Heat rejection fluid	Water, Water-NaK
Inlet coolant temperature	505 K

The reactor module uses a single high temperature gas-cooled reactor attached to the forward end of the spacecraft and coupled with redundant Brayton engines for power conversion, producing 200 kWe.

NUCLEAR COMPONENTS

The reactor core is a cylindrical uranium container with fuel elements arranged within the core structure. The fuel element components are a fuel filler, a gas gap to accommodate fuel swelling, a fission gas plenum to reduce pressure increase generated by fission process, a cladding liner to improve compatibility, and cladding to prevent fission gas leakage. The reactor operates in the fast spectrum because it allows lighter weight systems for Prometheus nominal power (Ashcroft and Eshelman 2007). Figure 13 shows a schematic of the fuel element.
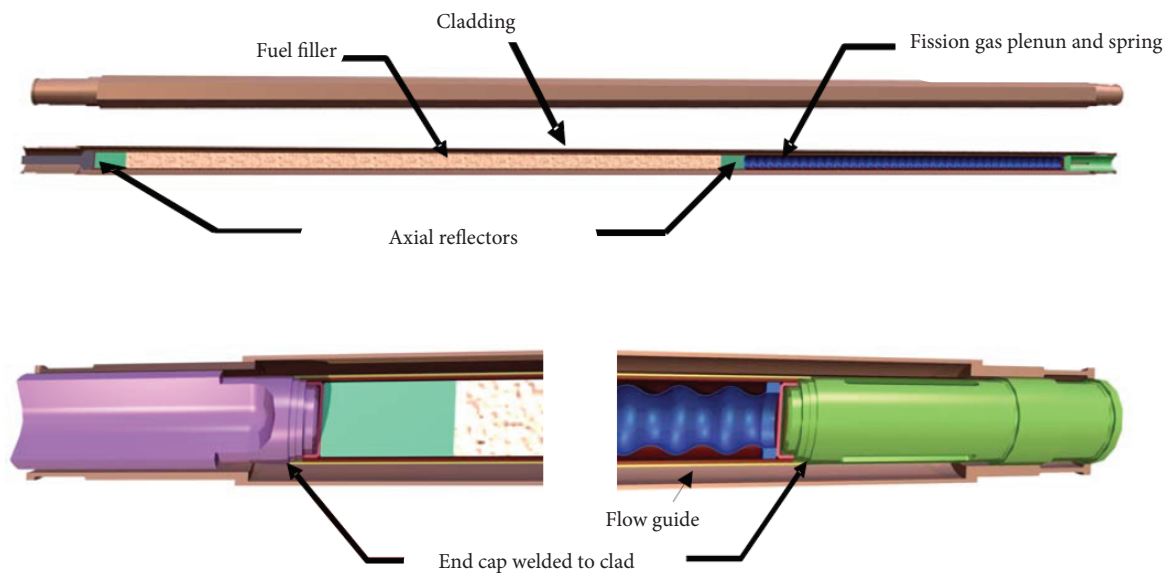
Figure 13. Fuel pin components (Ashcroft and Eshelman 2007).

The reactor vessel is cooled using a combination of the cooler reactor inlet gas and radiative cooling. Heat transfer between core and coolant occurs when the He-Xe mixture flows in between fuel elements, like represented by the arrows in Fig. 14. The turbulent flow inside the reactor vessel was simulated using CFD tools (Lorentz 2007), which indicated the appearance of regions where high velocities (which leads to higher pressure drops) and flow maldistribution take place, suggesting that new designs for reactor vessel would be necessary for hydraulic improvement.

Inlet   Outlet
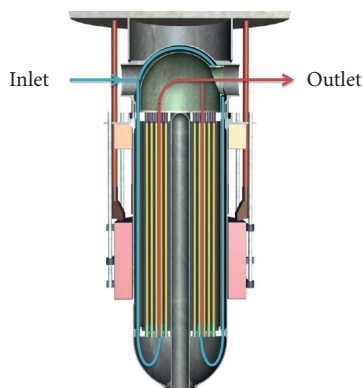
Figure 14. Reactor vessel section view. He-Xe flow is represented by the lines: blue ones are for fluid that has not flown through in between fuel elements, while red ones are for the fluid regions in fuel pins interstices.

The maximum fuel element temperature is 1300 K during normal full power operation, with low operating pressure (2-3 MPa). There is a control system to manipulate reflector motion according to reactor core needs. Control rods are used for criticality maintenance as well, but only during transport and launch, being withdrawn from the core prior to initial criticality. Last, radiation shield segment provides a conical shadow of reactor radiation attenuation to the remainder of the DSV.

There are several options for Reactor Core materials. Table 5 lists material options for reactor components and its main development concerns (Randall 2005).

Table 5. Materials envisioned for use in Prometheus.

Component	Material options	Concerns
Fuel	UO_2*	Swelling; Burn-up rate
	UN	Fission product chemistry; Porosity evolution
Reflector	BeO^*	Irradiation swelling; He gas release; Li_6 poisoning; Handling restrictions
	Be	
Neutron shielding	Water	Thermal management
	Be*	Handling restrictions
	B_4C*	
	LiH	Swelling vs. temp.
Cladding	Mo-47.5Re*	Radiation-induced embrittlement; Phase stability
	Si/SiC	Hermeticity; Fracture toughness; Conductive compliant layer
	Nb-1Zr	Creep capability; Radiation-induced and interstitial embrittlement
	T-111	Phase stability; Radiation-induced and interstitial embrittlement
	Ta-10W	Radiation-induced and interstitial embrittlement
	ASTAR-811C	Interstitial embrittlement; Phase stability; Fabricability

*Applied for base case.

Options evaluated for neutron shielding included LiH, water, Be and B_4C (see Table 5). Tungsten would be the best gamma shield material based on high density and moderate cost. LiH based neutron shielding would require Be/B_4C in higher fluence regions, but would provide a lower mass than concepts without LiH. A Be/B_4C shield would be considered a lower cost, lower risk option. Water shielding would be mass competitive with LiH.

The pre-conceptual base of Prometheus design using the described DSV geometry and Be/B_4C as shield material included a payload neutron radiation (DDD) of 5.10^{10} n/cm^2. The NOVICE radiation transport code was used for shielding modelling and calculation of the end of mission gamma (TID) exposures of the spaceship flight hardware. The baseline shielding design attenuated the TID levels to 0.5 Mrad (Si) in the Power Processing Units, 0.15 Mrad (Si) in bus electronics, and 0.15 Mrad (Si) in the telecommunications system (Randall 2005).
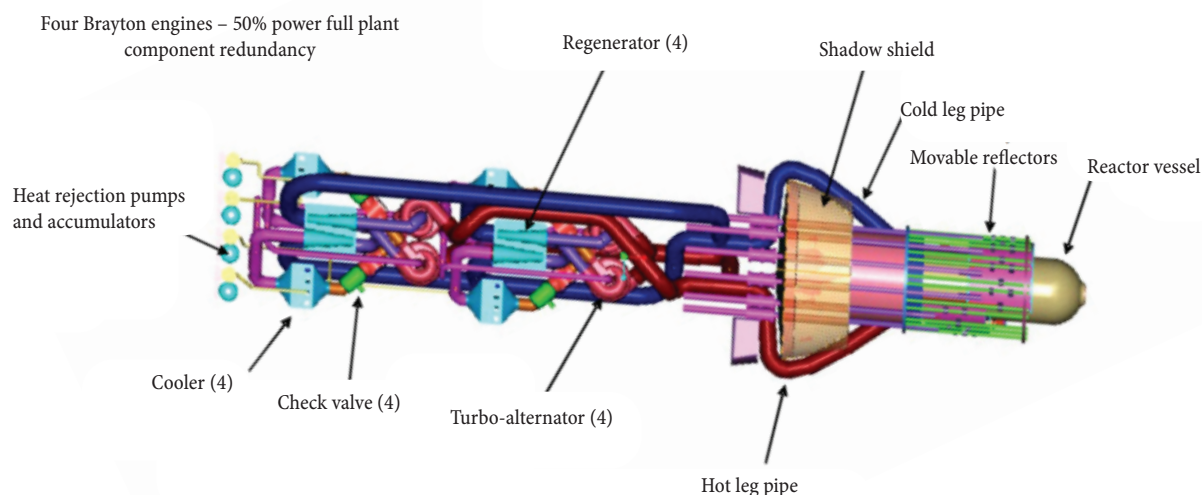
THERMOHYDRAULICS

An inert gas (a 39.94 g/mol helium and xenon mixture) is used to cool the core and transport heat to the Brayton engines. The chosen working fluid combines good thermal properties with no excessive number of turbomachine stages (El-Genk and Tourner 2008).

The gas core exit average temperature is limited to 1150 K, for availability of more usual materials on loop piping and pressure loading reduction on fuel element cladding or post-heated He-Xe (Ashcroft and Eshelman 2007).

Hot gas from the reactor starts the hot leg. It expands through a turbine, which is connected by a common shaft to a compressor and an alternator (converts turbine power into elec-tricity). It then goes to the recuperator, where heat is exchanged between the cold and hot legs. This mechanism pre-heats fluid that goes to the reactor, diminishing the hot source's power demand and consequently increasing cycle efficiency. Hot gas from the regenerator goes to the gas cooler, where heat is transferred to the heat rejection system radiators via a pumping loop using water or sodium potassium (NaK) as working fluid. It goes then to the compressor, where it is compressed using power from the turbine. After that, the gas goes to the recuperator and then back to the reactor, closing the Brayton cycle.

System cooling is provided by a heat rejection system formed by pumped loops using water/NaK as working fluids. This system is used to cool both reactor and shield, because modelling results revealed that this could be done without considerable shielding efficiency loss (Ashcroft and Eshelman 2007). These loops are coupled to the radiator panels, which provide heat waste through radiation.

Figure 15 shows a model of the Prometheus power plant. The total space nuclear power plant (SNPP) mass contribution is approximately between 7500 and 11000 kg, depending on the reactor type and plant configuration. Figure 16 is a block diagram

Figure 15. Prometheus reactor with four Brayton engines schematic (Ashcroft and Eshelman 2007).

of Prometheus thermohydraulics. Conversion efficiency depends on the number of Brayton units and the percentage operation power for each one, which is influenced by many factors, such as individual component and system reliability, overall system mass, tradeoffs between mass and reliability, and capability of the Brayton units to provide the required power and efficiency (Ashcroft *et al.* 2007). Table 6 shows performance data for pre-conceptual design, where there are four Brayton units, two at full operation and two spare. The power conditioning and distribution (PCAD) system conditions the three phase power outcomes from the Brayton unit to produce high voltage to the propulsion units and low voltage to the computers and instruments (Ashcroft and Eshelman 2007).
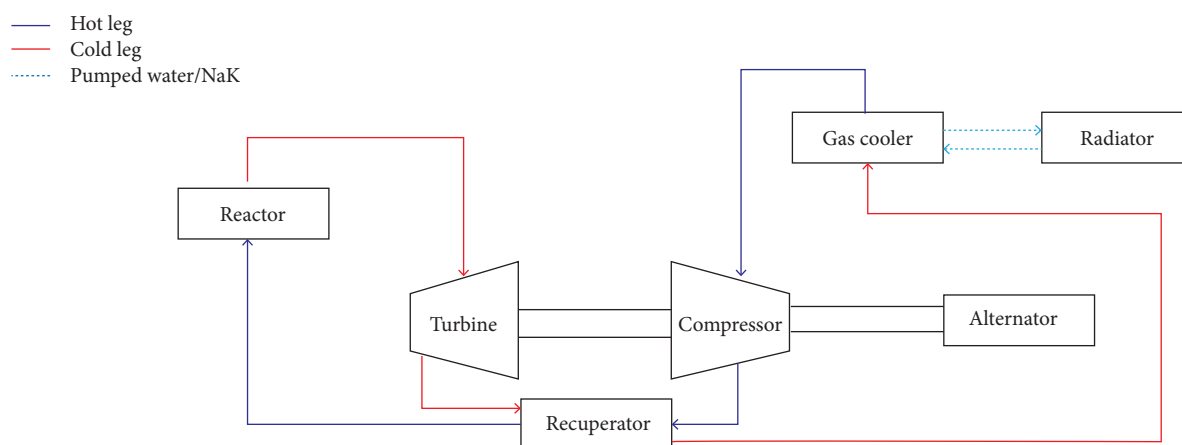
Figure 16. Block diagram of Prometheus thermohydraulics.

Table 6. Pre-conceptual design performance data (two 100 kWe Brayton units, two spare).

Parameter	Value
Converter efficiency	19.9%
System efficiency	18.2%
Reactor thermal power	1002 kWy
Turbine efficiency	90%
Turbine pressure ratio	1.83
Compressor efficiency	84.7%
Compressor pressure ratio	2
Recuperator effectivity	92%
Recuperator thermal power	757 kWt
Gas cooler effectivity	94%
Gas cooler thermal power	382 kWt
Radiator thermal power	767 kWt
Alternator efficiency	91.2%
Alternator electrical power	196.6 kWe

SPACECRAFT AND MISSION MODULES

The configuration of the Spacecraft Module is dominated by the ~43 m long main boom assembly with radiations panels mounted on it for heat rejection. The main boom configuration also provides distance between reactor module and the electronic components housed in the bus segment, located at the after end of the spacecraft. It contains the majority of the electronic subsystems needed to control and operate the DSV.

The spacecraft boom size was calculated from a trade-off optimization between system mass, heat rejection and reactor radiation protection, based on thermal and shielding models of the DSV.

Ion and Hall thrusters provide spacecraft propulsion, making up the Electric Propulsion Segment of the Spacecraft. The docking segment is included in the Spacecraft Module to support early on-orbit operations and docking with interplanetary transfer stage. It provides power, communication and attitude control for the DSV in post-launch through deployment and commissioning (Randall 2005).

The Mission Module is consisted of instruments and supporting elements that are mounted to the DSV, primarily in the area of Spacecraft Bus. It is unique for each mission.

FISSION SURFACE POWER – FSP (2006)

PROJECT HISTORY

The FSP program was initiated in 2006 as the Prometheus program was phased-out. Its objective is to develop technology to provide the option for fission surface power to the US Space Exploration Policy at a reasonable cost with added benefits over competitive options (Palac et al. 2011).

In 2006, NASA and DOE implemented the Affordable Fission Surface Power System Study (AFSPSS), which included cost analysis and research of possible approaches to minimize costs while meeting mission performance and lifetime requirements. A government study team with members from NASA and DOE evaluated technology options and design variables, electing a concept based on affordability and risk (FSPT 2010).

A NaK-cooled, UO_2 fueled reactor coupled to free-piston Stirling converters and a pumped-water rejection loop concept was selected (Poston et al. 2009). This selection prioritized lower-risk over lower mass or higher system performance and was followed by a development schedule and a Work Breakdown Structure (WBS).

One of initial steps stablished by FSP team was the development of a Balance-of-Plant (BOP) demonstration, called Techno-logy Demonstration Unit (TDU), to bring FSP to Technology Readiness Level (TRL) 6. This experiment and its highlights will be exposed forward.

TECHNOLOGY OVERVIEW

From 2008 to 2010, the fission surface power research emphasized concept definition technology development. The FSP reference concept for the lunar surface is consisted of four major elements: Reactor, Power Conversion System (PCS), Heat Rejection System (HRS) and Power Management and Distribution (PMAD).

The reactor module is buried 2 m deep in the ground with an upper plug shield to protect equipment from radiation. The reactor generates nuclear heat through fission, which is transported to the PCS. Electrical power produced by the PCS is processed through the PMAD to the User Loads. Other PMAD functions are: provide power for Power Conversion startup and for auxiliary loads associated with the Reactor and Heat Rejection, and provide the primary communications link for command, telemetry, and health monitoring of the FSP system (Koroteev et al. 2015). The waste heat is rejected by radiation using the HRS.

There are NaK pumps, Stirling convertors and water pumps mounted on a 5 m tall truss structure that attaches to the top face of the shield, as shown in Fig. 17. The center structure has two symmetric radiator wings attached to it. The FSP design is a 40 kWe system with 8 years lifetime suitable for lunar and Mars surface applications, with low temperature and low development risk.
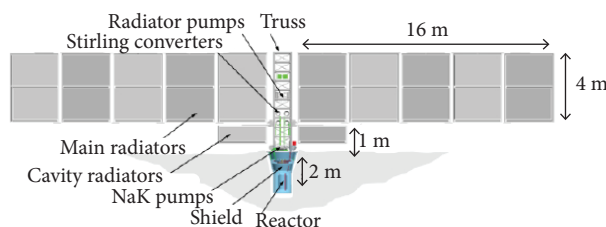
Figure 17. FSP Technology Concept (Mason and Houts 2010).

MATERIALS SELECTION

Fuel decision upon reactor is highly dependent on the specific mass and lifetime. UO_2 and metal fuels (UZr and UMo) were considered low-cost/risk options, when specific mass was not a major driver. Metal fuels had been widely used in research reactors. Besides, the majority of space reactors launched (Russian BUK) had used metal fuels. However, UO_2 fuel can support clad temperatures of around 950 K. Besides, low power (< 200 kWe) and burnup alleviates the need for UO_2 development. After a throughout comparison between UO_2 and the metal fuel U-10Zr, the first one was chosen, recognizing that U-10Zr and UZrH could be affordable alternatives depending on final requirements.
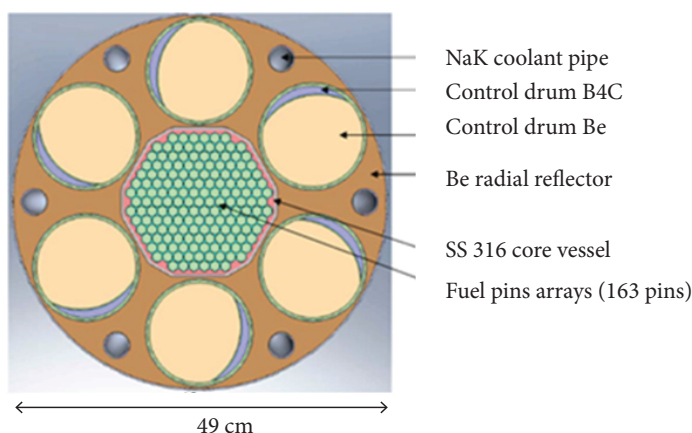
316 Stainless Steel 316 L was chosen for the FSP reference reactor system structure (mostly notably fuel cladding) material. 316 and 304 steels are regularly produced and can support peak temperature < 900 K, do not experience a significant negative change of properties if irradiated in < 1 displacement-per-atom (dpa) and do not suffer changes in strength, creep, ductibility, fracture toughness or fatigue resistance in FSP nominal power and lifetime (Poston *et al.* 2009).

The concept for the liquid metal pumps used in the heat rejection is the most important reactor technology selection. Electromagnetic (EM) pumps were chosen instead of mechanical, for presenting some decisive advantages: there are no shaft seals; they have no moving parts other than the liquid metal itself and therefore are free from wear and require no bearing lubrication. EM pumps can be divided into induction or conduction pumps. The induction pump concept may be further categorized by configuration: annular, flat and helical; and the conduction pumps are either AC or DC powered. Based on prior experience (Mason 2010), an Annular Linear Induction Pump (ALIP) was selected for the FSP reference. This concept is the lowest mass of the induction pump family and has the simplest duct design (Poston *et al.* 2009).

NUCLEAR COMPONENTS

The FSP reference reactor was designed to deliver ~185 kWt to the PCS via pumped NaK coolant. Many design decisions were made to simplify core neutronics and dynamic response. The fast spectrum in the core makes the use of point kinetics (which evaluates transient reactor flux/power response in a lumped parameter model) has little uncertainty, which also makes power input to TDU much easier, making non-nuclear testing more realistic.

Figure 18 shows a plan view of the FSP reference reactor and Fig. 19 shows a 3D section view of the FSP reference reactor with indications of coolant flow inside the core.

NaK coolant pipe
Control drum B4C
Control drum Be

Be radial reflector

SS 316 core vessel
Fuel pins arrays (163 pins)

49 cm

Figure 18. Plan view of the FSP reference reactor (Poston et *al.* 2009).

There are 163 fast spectrum UO_2 fuel pins inside the core, each one of them with appropriate SS-316 cladding (Briggs *et al.* 2014). The fuel is assumed to have 94% density, with 63% enriched uranium oxide. Each Coolant flow is represented by the blue and red arrows (Poston *et al.* 2009). Fuel pin contains BeO pellets at each end of the fuel to serve as an axial reflector, and there is a small gap at the top of the pin, which also serves as a fission gas plenum.
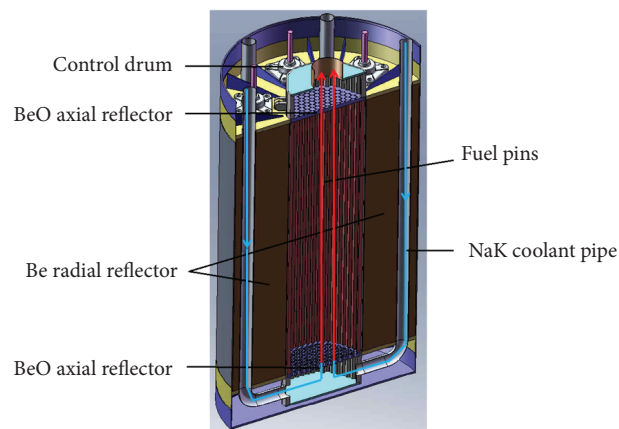
Figure 19. 3D view of the FSP reference reactor (Briggs *et al.* 2014).

The reference core uses a triangular pitch pin-lattice arrangement. The pins are fixed axially and radially on one end, but can float axially on the other end. The dodecahedron vessel is used to allow radial reflectors and control drums to be closer to the fuel, allowing better reactivity control. The radial reflector is Be metal in a SS-316 can. Be was chosen rather than BeO for being less susceptible to radiation/temperature induced swelling and cracking. The control drums are composed of the same materials (Be in a SS can), with a 112° banana-shaped arc of B_4C absorber to provide control (see Fig. 17). Each drum is baselined to be powered by a dedicated motor and drive mechanism.

Coolant flow is fed from the top of the reactor to the bottom via piping that travels through the radial reflector, which allows ex-lattice flows and hydraulic diameter to be larger, minimizing pressure drops, and brings radial reflectors and control drums closer to the core. Coolant flow is highly turbulent (Re 15000), and the temperature drop in the coolant is low, so the design is tolerant to thermal-hydraulic changes caused by pin movements (Poston *et al.* 2009).

Radiation Shielding was not yet fully designed, because it depends heavily on reactor architecture. More details about radiation shielding can be found in Poston *et al.* (2006).

HEAT TRANSPORT

The pumped NaK heat transport system (HTS) is responsible for delivering reactor thermal power to the Stirling engines. It is consisted by the piping, pumps, accumulators and intermediate heat exchangers (IHXs), which in this case are of the shell-and-tube type. This system is coupled to the Stirling hot head via the NaK-to-He heat exchanger.

Figure 20 shows a notional layout of the FSP heat transport system. The reference system contains two 50% power intermediate loops. This configuration mitigates the risk of He-to-NaK breach at the Stirling heater head, provides a buffer between the primary NaK and the Stirling convertors, and allows NaK flow rate to be adjusted separately from the reactor (Mason 2010).
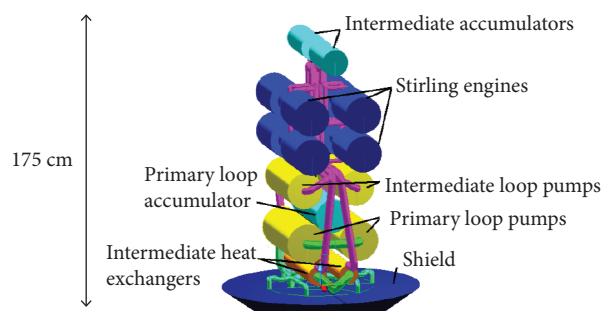
Figure 20. Notional layout of FSP component above shield (Poston *et al.* 2009).

The primary NaK coolant flows up the core through the interstitials between the fuel pins. Flow then exits the upper plenum into a single pipe that goes straight through the upper shield. The primary flow then splits into two 50% pipes, which pass in parallel through the IHXs (tube side) and then recombine into a 100% flow pipe, flowing through the 2 primary pumps in series. After passing by the accumulator, the flow is divided into 6 smaller pipes that go back to the shield. These pipes then neck down, continue straight through the radial reflector and then bend inward to feed reactor lower plenum.

Intermediate loop NaK proceeds from the shell side of the IHX and splits into two 50% flow pipes that go to 2 parallel Stirling engines. The two fluids flow through the Stirling heater heads and recombine into a full flow pipe, which passes by the intermediate volume accumulator. The flow passes through the intermediate loop pump, then back to the shell inlet of the IHX.

The preferred configuration for the NaK-to-NaK IHX has the primary flow through the tubes and the intermediate flow through the shell for shielding and reliability regions. Like shown in Fig. 19, the accumulators are horizontally oriented, which shortens the axial profile of the component stack and allows NaK in the primary accumulator to be properly shielded by the intermediate pumps and accumulators. Table 7 shows main design parameters of reference system Heat Transport System.

Table 7. Fission surface power HTS data.

Parameter		Value
Maximum pressure		140 kPa
Maximum temperature		850 K
Primary loop	Thermal power	185 kWt
	Number of pumps	2
	Pumping power per pump	~ 850 We
	Number of accumulators	1
	Flow rate	4.3 kg/s
	Hot temperature	850 K
	Cold temperature	800 K
	Pressure drop	20-25 kPa
Intermediate loops (per loop)	Thermal power	93 kWt
	Number of pumps	1
	Pumping power	~ 300 We
	Number of accumulators	1
	Flow rate	3.5 kg/s
	Hot temperature	820 K
	Cold temperature	790 K
	Pressure drop	9-12 kPa

POWER CONVERSION AND HEAT REJECTION

Figure 21 shows a block diagram of the FSP reference concept. Red and yellow arrows respond for, respectively, the primary and the intermediate pumped NaK loops, which were already mentioned in the previous section. The use of redundant components and parallel fluid loops allows the system to produce partial power in the event of unexpected failures (Mason 2010).

Each Stirling convertor (Stir in Fig. 21) is consisted of two axially opposed Stirling heat engines and two linear alternators, which deliver 6 kWe each at 100 Vac to the Power Management and Distribution (PMAD) subsystem, where AC output is converted into DC and distributed to the user loads and to the internal power demanding systems.
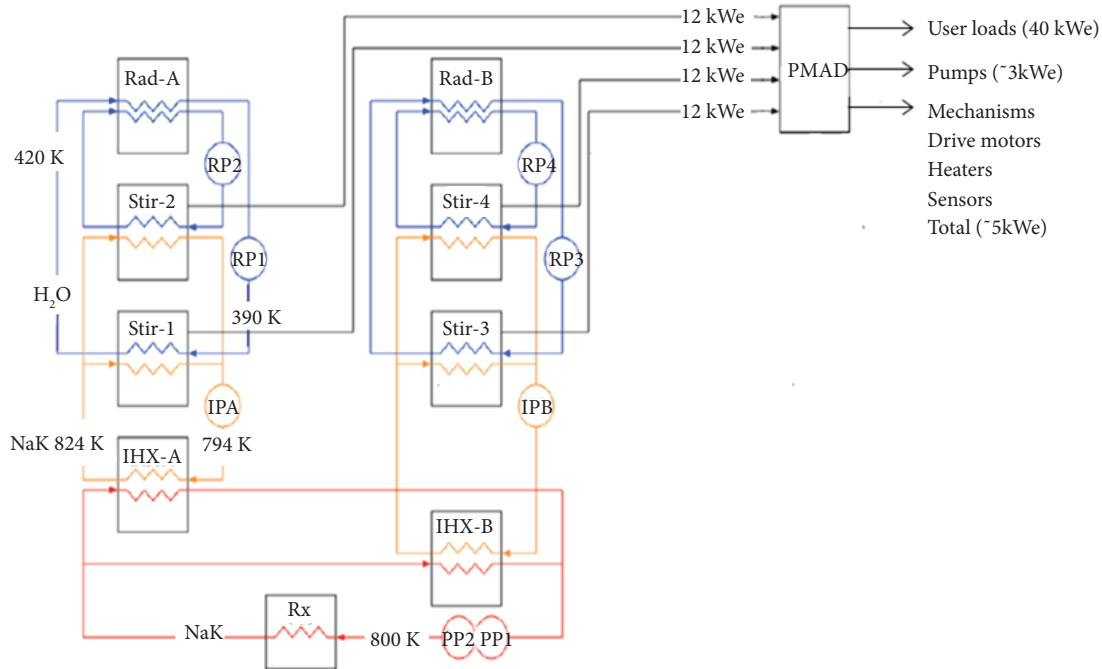
Figure 21. FSP Preliminary Reference Concept Schematic (Mason 2010).

The 48 kWe electrical power that comes from the Stirling convertors serves as a supply to the pumps (~3 kWe) and system parasitic loads (~5 kWe), and still delivers 40 kWe net for user loads.

The heat rejection subsystem (HRS) is consisted of four water heat transport loops and two radiator (Rad in Fig. 21) wings (two loops per wing). The radiator wing receives heated water at 420 K from the Stirling convertors and returns the water at 390 K using a mechanical radiator pump, while rejecting approximately 35 kWt for each water loop. The resulting Stirling cold-end temperature is 425 K. The total heat load is ~140 kWt and the total two-sided FSP system radiator area is 184 m² assuming a 250 K effective heat sink temperature. Each radiator includes 10 sub-panels, each measuring approximately 2.7 m wide by 1.7 m tall (Mason 2010). Table 8 compiles main information about PCS and HRS design parameters.

Table 8. Fission surface power PCS and HRS data.

Parameter	Value
System efficiency	26%
Stirling machines thermal power	46.5 kWt
Primary loop IHXs heat transfer	93 kWt
Radiators heat transfer	70 kWt
Radiator wing area	92 m²
System electric power output	48 kWe
User loads	40 kWe
Pumps electric power demand	3 kWe
HRS loops mass flow	0.28 kg/s
HRS pumps pressure drop	385 kPa
Stirling hot temperature	778 K
Stirling cold temperature	425 K

TECHNOLOGY DEMONSTRATION UNIT (TDU)

The TDU is a system level demonstration of the technologies used in the AFSPSS, designed to deliver 25% of FSP power. The initial concept was composed of a reactor simulator (RxSim), a Power Conversion Unit (PCU), and a Heat Rejection System (HRS) in a thermal vacuum facility. The primary objective of the TDU is to demonstrate the technology readiness of the integrated FSP system using a non-nuclear heat source.

TDU Initial Concept

The RxSim initial concept is consisted of a core simulator, a primary NaK transport loop, a NaK-to-NaK heat exchanger and an intermediate NaK heat transport loop. The core simulator includes a series of electrical resistances to represent the reactor heat source, and the NaK loops each include electromagnetic pumps and volume accumulators. The RxSim Controller collects data, relays command signals, and supplies electric power for the RxSim components. It also controls NaK outlet temperature and flow rate in both loops and simulates the expected temperature-reactivity of a FSPS reactor.

The PCU generates electric power with the heated liquid metal and rejects waste heat to the HRS, which includes a pumped water cooling loop coupled to vertical radiator panels suspended in a thermal vacuum facility. For the initial concept, both Brayton and Stirling were under consideration, where Brayton would utilize a single heat engine, a rotating turbine-alternator-compressor and a gas-to-gas recuperator, and the Stirling option would utilize two free-piston heat engines with integral regenerators and linear alterna-tors in an opposed configuration to maintain a balanced motion (Palac *et al.* 2011). The PCU Controller collects data, relayscommand signals, supplies electric power for converter startup, processes electric output (making AC-DC conversion), and regulates parasitic load control and voltage.

The Facility Cooling System (FCS) rejects waste heat from the thermal vacuum facility utilizing an external heat exchanger.

The HRS system is composed of a radiator, a pumped water transport loop, and a HRS controller. The water loop cools the PCU and includes a pump and a volume accumulator. Heat exchangers transport heat from the pumped water loop to the heat pipe evaporators. The two radiators are sided vertical panels with embedded titanium-water heat pipes. Heat is conducted to the condenser sections of the heat pipes and then to the panel surface where it is conducted by radiation to the walls of the thermal-vacuum chamber.

The PMAD system and the data acquisition and control are external to the thermal vacuum facility and use commercially available, rack-mounted components.

The nuclear aspects of the FSPS are not demonstrated in the TDU, but those are considered fairly mature based on terrestrial reactor technology, although some nuclear-related tests will be conducted in parallel with TDU, such as reflector control drive testing, shield development, and material/component irradiation testing. The TDU does not demonstrate system lifetime or launch/landing survivability, which can be better described in a subsequent mission flight development program. The major challenges of the TDU are the liquid metal heat transport, the electric power generation, and the waste heat removal.

Figure 22 is the block diagram repre-sentation of the TDU energy flow. The NaK loops are represented by the red arrows and water loops by the blue arrows. Figure 23 graphically compiles main performance requirements for the initial design of TDU system with a Stirling PCU. Figure 24 shows a 2D representation of the TDU and Fig. 25 shows a 3D representation of the TDU test layout inside the Thermal Vacuum Facility.

TDU Tests

The initial TDU design would simulate a single leg of the baseline FSP using an electrically heater core simulator, a primary and a secondary liquid metal loops, a single Stirling PCU, and a pumped water loop which rejected heat to six titanium-water heat pipe radiators.

This concept was intended to demonstrate the balance-of-plant of the FSP to TRL 6. However, budget reductions and organizational changes had reduced the TDU scope. The secondary loop, radiators and power conditioning were removed and the TRL goal was reduced to 5. In addition, testing was focused on system performance, removing several transient system scenarios
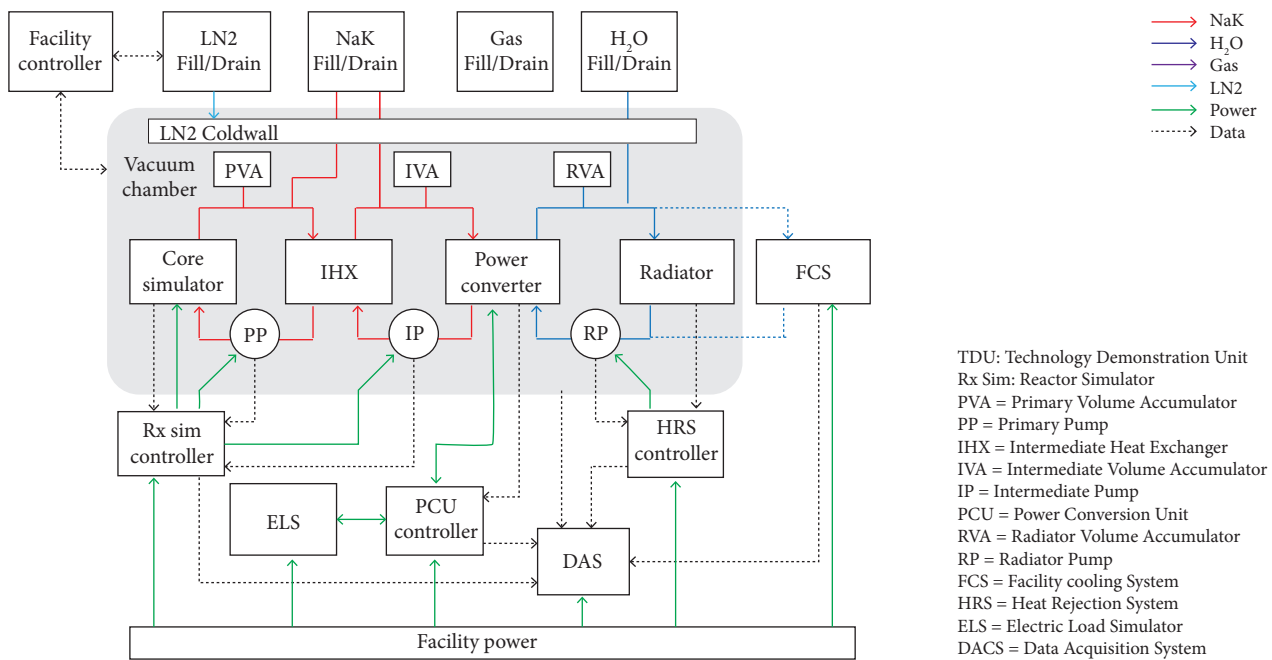
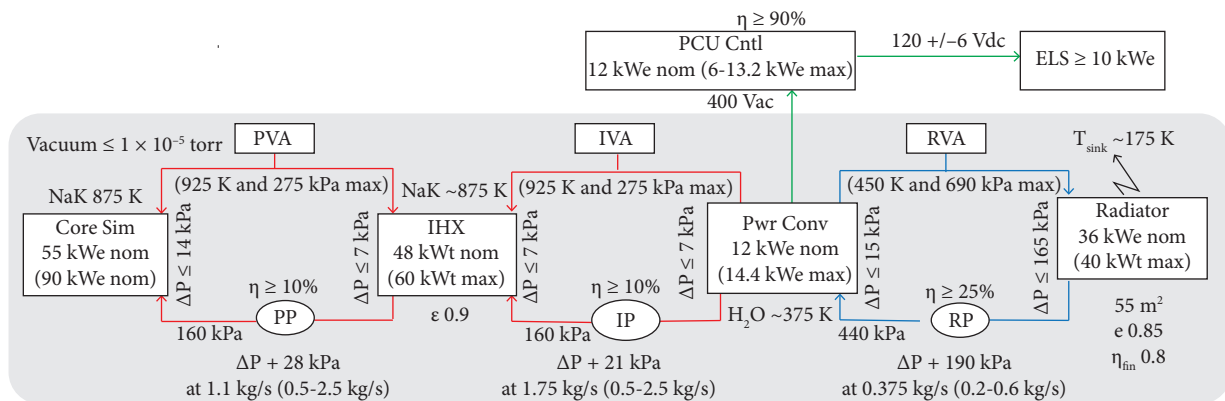**Figure 22.** TDU Initial Concept Block Diagram (Mason 2010).

Legend:
- NaK
- H₂O
- Gas
- LN2
- Power
- Data

TDU: Technology Demonstration Unit
Rx Sim: Reactor Simulator
PVA = Primary Volume Accumulator
PP = Primary Pump
IHX = Intermediate Heat Exchanger
IVA = Intermediate Volume Accumulator
IP = Intermediate Pump
PCU = Power Conversion Unit
RVA = Radiator Volume Accumulator
RP = Radiator Pump
FCS = Facility cooling System
HRS = Heat Rejection System
ELS = Electric Load Simulator
DACS = Data Acquisition System

Figure 23. TDU initial concept key performance requirements (Mason 2010).
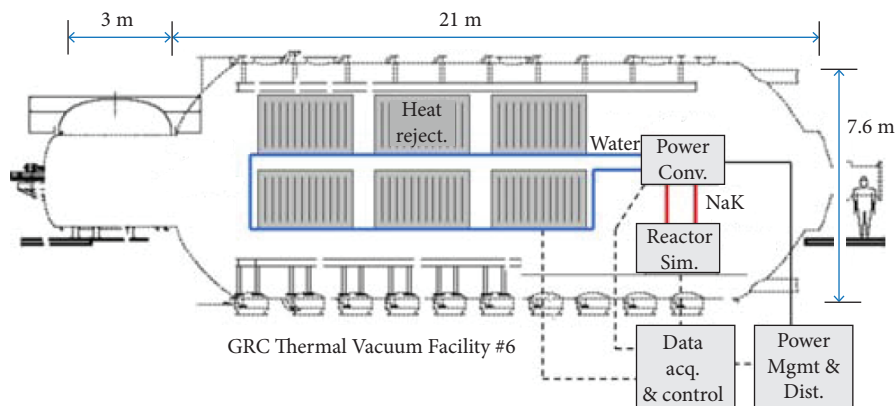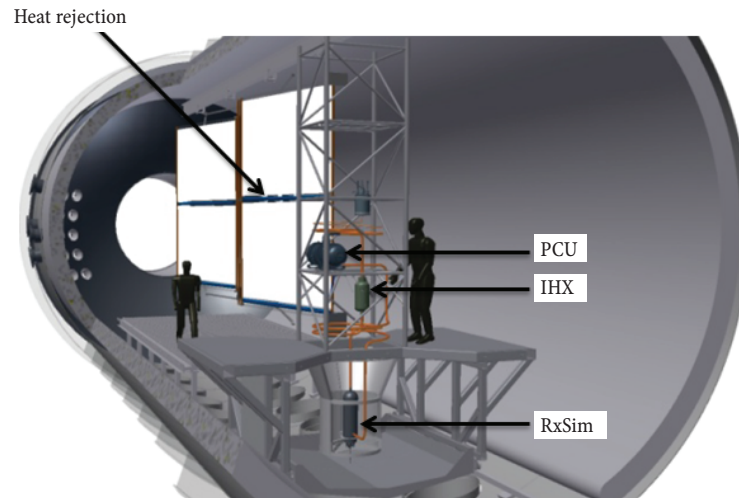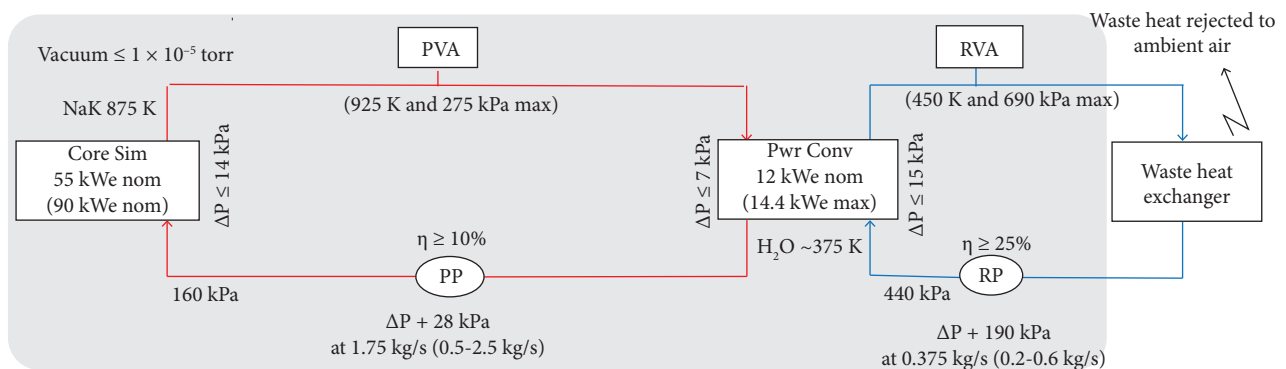

Figure 24. TDU test layout 2D view (Mason 2010).

from the original test matrix (Briggs *et al.* 2016). TDU assembly and testing was performed in GRC between 2014 and 2016. The tested TDU schematic is shown in Fig. 26.

Figure 25. TDU test layout 3D view (Briggs *et al.* 2014).

Figure 26. Schematic of the TDU as-built configuration (Briggs *et al.* 2016).

Several component and subsystem level tests were performed before experimentation of fully mounted TDU assembly. The TDU component tests included two ALIP and RxSim tests at MSFC, subscale Stirling tests at GRC and MSFC, testing of full-scale Stirling PCU at Sunpower Inc, and testing of radiatior panels and subsystem testing of both liquid metal and water loops at GRC.

ALIP testing at MSFC lead to a 5% pump efficiency compared to an expected value of 10% at the nominal conditions of 850 K, 1.75 kg/s and 28 kPa liquid metal loop pressure drop. However, redesign and fabrication of a new pump was outside the scope, so the existing ALIP was used as-built for TDU tests.

Liquid-metal subsystem testing revealed an issue with one of the two ALIP power supplies. It was replaced, but TDU test schedule did not allow further testing, so liquid metal mass flow was limited to 1.2 kg/s.

PCU testing at sunpower showed that, operating at nominal conditions (850 K hot-end temperature, 375 K water temperature, 0.375 kg/s water flow rate) produced 12.2 kW of power at a gross efficiency (electrical power output divided by electrical power input to the electric heaters) of 25.5%, compared to the specified values of 12.0 kW power and 26% efficiency. The electrically heated head was then replaced with a heater head that included a liquid metal heat exchanger for testing in the TDU. This final configuration was then shipped to GRC for system-level testing, where it was integrated into the existing water and NaK subsystems. Figure 27 shows the TDU experiment in GRC Vacuum Facility 6.
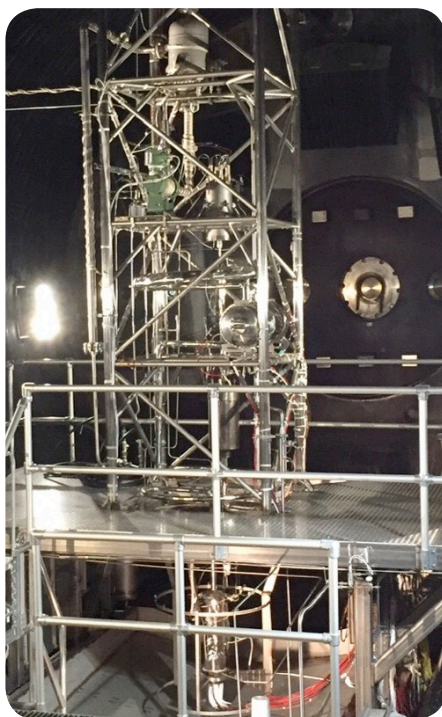
Figure 27. FSP TDU installed in Vacuum Facility 6 at GRC (Briggs *et al.* 2016).

The PCU power output measured during NaK testing was universally lower than the PCU power output measured in Sunpower tests, suggesting that there may not have been adequate thermal contact between the NaK heat exchanger and the internal acceptor.

Tests with cold-end at 360 K resulted in the excessive helium leakage of the PCU into the vacuum chamber; therefore, future tests will be limited to a minimum cold-end temperature of 375 K. The effect of increasing the hot-end by 25 K is shown to be similar to the effect of decreasing the cold-end temperature by 15 K in both PCU and system level performance. PCU performs better at high water flow rates, but these gains are nearly eliminated on the system level due to increased pump power.

In its final configuration at nominal operating conditions, the PCU produced 8.9 kW of power at an efficiency of 21.7%, resulting in a net system power of 8.2 kW and a system level efficiency of 17.2 percent. The maximum PCU power of 10.4 kW was obtained in maximum NaK temperature of 875 K, minimum water temperature of 350 K, 1.1 kg/s liquid metal flow and 0.39 kg/s water flow at an efficiency of 23.3%, resulting in a 9.6 kW system net power and 18.7% system efficiency. These values compare favorably to the original system level performance specifications of 10 kW power output at 18% system efficiency (Briggs *et al.* 2016).

After finishing the nominal cold-end temperature part of the test matrix, the TDU was taken to its high cold-end temperature condition. In the transient testing, helium working fluid contained within the PCU started breaching into the water cooling loop. This caused an emergency shutdown sequence in which the engines were stalled, the core simulator was turned off, the residual water was vented through the drain leg and a nitrogen flow was initiated to provide auxiliary cooling to the PCU. The PCU was not able to hold helium charge pressure and TDU testing could not continue. There is currently no funding available for the PCU repair. The TDU Test Team suspects that this leak occurred in one of the elbows of the water manifold leading to the heat rejector. Redesign of PCU components and/or improvement in fabrication methods are required to avoid similar failures in the future.

Other potential areas for improving system performance or the quality of test data in subsequent programs or follow-on testing include improving ALIP design to achieve performance in line with previously built pumps, improving design of the water-helium boundary on the Stirling engine, processing the engines in a way that allows the Stirling engines with NaK heads to be tested and modified prior to the installation of the test loop, including heat pipe radiators for accurate system response and transient feedback, improving reactivity feedback software to allow accurate transient reactor simulations, and adding power conditioning and prototypic engine control electronics to more accurately reflect mission demands.

DEMONSTRATION USING FLATTOP FISSION – DUFF (2012)

PROJECT HISTORY

Since 1965, NASA has made significant progress in larger fission power system (FPS) development for surface and in-space applications but did not made effort in flight qualifying such systems, mostly due to development cost and uncertainty of a near term mission pull. There was a portfolio gap between non-flight qualified higher power (> 10 kWe) FPS and flight qualified small Radioisotope Power Systems (< 1 kWe). A 1-10 kWe FPS called Kilopower was a possible option for filling this gap (see Fig. 28).
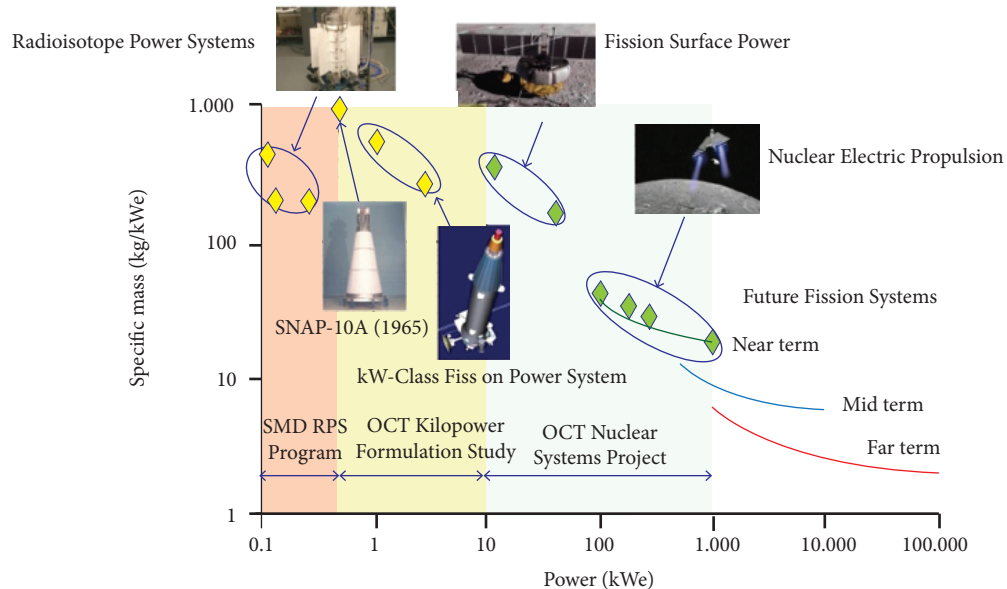

Figure 28. Space nuclear mass-to-power performance map (Mason *et al.* 2013).

LANL and GRC had proposed several concepts for space applications. One of the most promising approaches used a compact fast reactor, cooled by heat pipes and transferring power to Stirling engines. The proposed concept is shown in Fig. 29. This system was designed to produce 800 W of electricity and reach hot end temperatures of up to 800 °C.
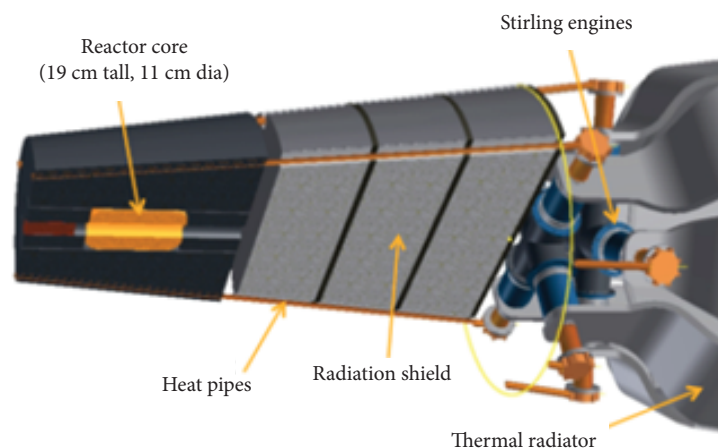
Figure 29. Proposed HP cooled – Stirling Engine Reac-tor for Space Applications (Poston *et al.* 2013).

Figure 30 is a drawing of its nuclear subsystem. It is composed by an enriched uranium cylindrical core surrounded by a beryllium reflector. A single rod of boron carbide is used for reactivity control, and eight super-alloy-sodium heat pipes connect the core to the Stirling convertors that supply electricity for the spacecraft. The engines are cooled by a water heat pipe coupled to a thermal radiator. The shield lies between the reactor core and the Stirling Engines (Poston *et al.* 2013).
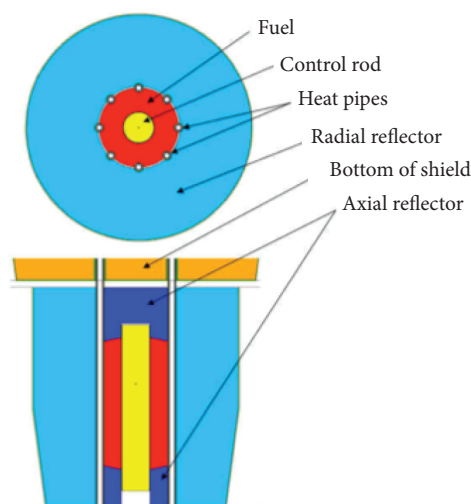
Figure 30. Kilopower proposed Nuclear Subsystem (Poston *et al.* 2013).

There had to be a ground test to give a better understanding of this mechanism and to demonstrate the feasibility of this concept, considering that the last FPS flight had occurred 50 years before. Therefore, representatives from the LANL, GRC, and SunPower Inc. performed the Demonstration Using Flattop Fission (DUFF) in the dependences of the Device Assembly Facility (DAF) at the Nevada Nuclear Security Site (NNSS) to give technological support to the Kilopower concept. The experiment did two test runs (on September 13th and September 18th) and it was notable for taking less than a week and less than a million dollars to be developed.

Most of the American space nuclear power systems in the last decade (SP-100, JIMO, and FSP, for instance) included a large scope with ambitious objectives (systems using high temperatures with unproven technology and exotic materials). DUFF strongly differed from previous power systems for being a lower cost, smaller concept with the specific goal of generating electricity from nuclear fission.

The first discussion about a new reactor concept applicable for space started in the Mars Science Laboratory launch. A plan of a less-than-year working demonstration was presented in early February 2012 to a group of interested parties in LANL. The presentation was well received, and a proposal for NASA submission was suggested, but it wasn't done because of the innumerous uncertainties that were attached to it: the last space reactor system had been launched half a century before, none of the one hundred US research reactors had been undertaken since the formation of DOE and none of existing reactors at DOE facilities had been used to produce electricity. NASA probably wouldn't agree to provide funding. Instead, LANL decided to take the reactor design on internal funding, demonstrating its interests to the other parties (Dixon *et al.* 2013).

After NASA joined into the project, the two agencies took the project to Nevada Nuclear Security Site (NNSS) in March, with representatives from LANL, GRC, MSFC, and JPL in attendance. Until this point, no funding was applied on the project. NNSS representatives authorized testing at their site and committed to covering their staff costs and support of the test. Actually, each institution funded its own internal costs. This was a key feature for project success, as it diminished bureaucracy. By May, most of the funding needed to complete the experiment was in place, so the project executions could be started.

MATERIALS AND PROCEEDINGS

Following the concepts of the Kilopower reactor, a water heat pipe would be inserted inside a ^{235}U fuel core to conduct the heat to a pair of Stirling engines, which would convert heat into electricity. A light would be powered by the Stirling engines, completing the proof of concept.

The first plan included manufacturing experiment fuel and reflector, which changed to using the existing structure: a Flattop nuclear assembly in NNSS. It included a highly enriched uranium (HEU) spherical core on a natural uranium pedestal. It was very similar in size and dimension to the reference concept, and it had been previously tested to pedestal temperatures of up to 300 °C (Dixon *et al.* 2013). It was a highly reflected, fast-spectrum system.

The Flattop also had a 1.2827 cm diameter hole through its center. GRC had been performing life testing of 1.27 cm diameter heat pipes in temperatures of up to 300 °C, so one of these pipes was sent to Nevada. Actually, it was not the heat pipe used in the DUFF experiment, but it facilitated the experiment from a technology standpoint.

The HEU core was surrounded by a semi-spherical and two quarter-spherical natural uranium reflectors. The device also had control rods inside the reflectors to keep nuclear fission reactivity under control.

To make sure the fuel would not be damaged or the heat pipe would not become lodged in the fuel, graphite lubrication was applied between the heat pipe and fuel, and the temperature drops caused by this lubrication were be tested during GRC laboratory testing (Gibson *et al.* 2013).

Another concern is that the heat pipes should be as adiabatic as possible, minimizing heat loss to the reflectors. To meet this requirement, the heat pipes were involved by stainless steel sleeves (SS and alumina were tested) that would provide an air gap between heat pipes and reflectors, minimizing heat transfer. The heat pipes needed a pumping capacity in the wick structure due to its horizontal orientation (no gravity effect) and high heat flux. These requirements were satisfied by using a nickel sintered wick with integral arteries as shown in Fig. 31 (Gibson *et al.* 2013).

0.500 in. 316L SST Tube
0.049 in. wall

0.060

Nickel powder wick 100,200,325 mesh

Ø.046 ×8
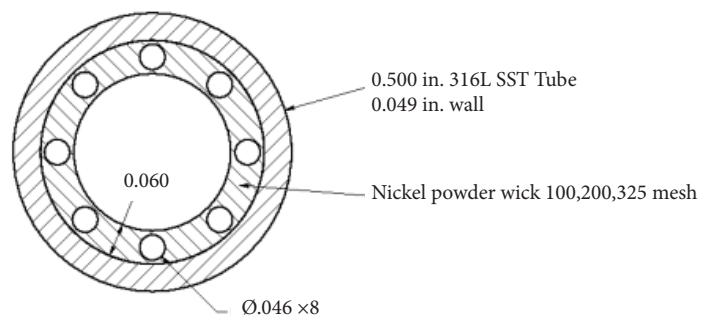
Section E-E
Scale 6:1

Figure 31. Section of heat pipe (Gibson *et al.* 2013).

Sunpower Inc. provided an existing set of Stirling converters suitable for low temperature operation, the Buzz converters. GRC designed and fabricated a copper block for mating the engine pair to the heat pipe. This block also had a hole for a 1.27 cm heat pipe. These engines were specifically designed for low temperatures, being able to operate at –30 °C on the cold end and up to 400 °C on the hot end, and pressure ratios between 1.55 and 1.92. They could also provide positive power at 150 °C hot end temperature, while others would need a minimum 200 °C. Figure 32 shows the two Stirling engines with white pistons coupled to alternators and connected by the copper block.

The Flattop core mass was ~18 kg vs. ~25 kg for the flight system (Poston *et al.* 2013). The used Flattop configuration is shown in Fig. 33. Figure 34 is a draft of the Flattop experiment.

Since Flattop was a national asset, the temperature of the experiment was limited to 300 °C, which required the usage of water heat pipes, a chiller to maintain cold-end temperatures below the tolerance and Stirling convertors that could operate at these temperatures. The working fluid for heat pipe design highly depends on its operating temperature. The flight reactor, designed to reach 800 °C, would use liquid sodium instead of water.
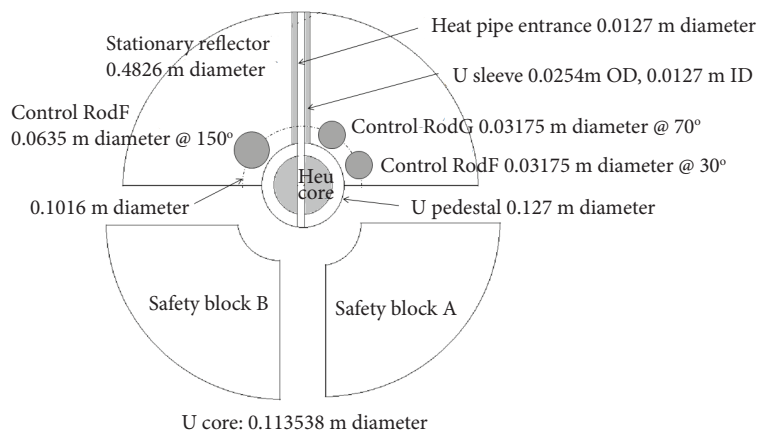
GRC prepared conversion hardware while LANL worked through the nuclear design. After experiment setup, the tests started at NNSS Device Assembly Facility on September 13th.
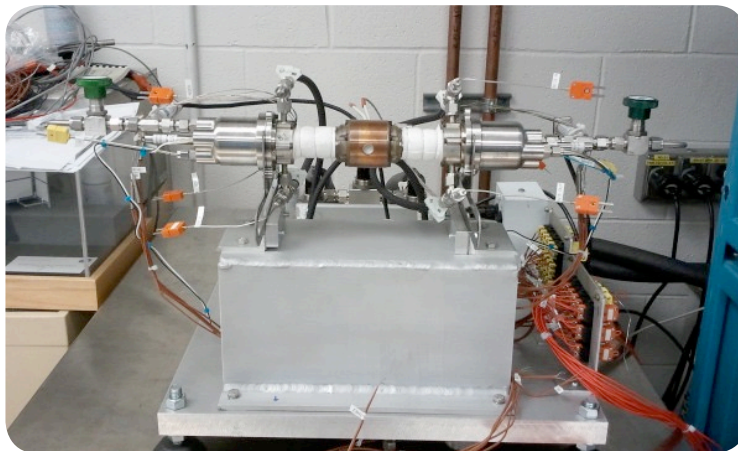
Figure 32. Buzz Stirling engines used for DUFF experiment (Gibson *et al.* 2013).
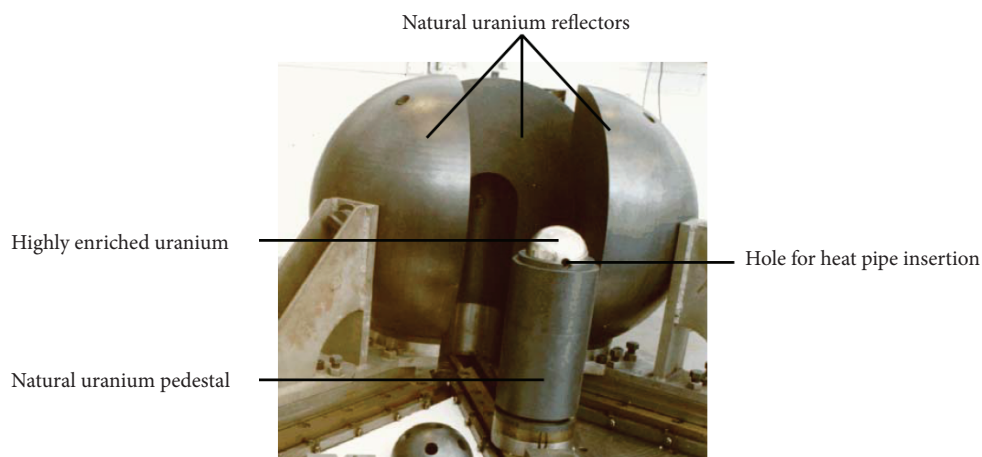
Figure 33. Flattop critical experiment assembly (Poston *et al.* 2013)

**Figure 34.** Flattop reactor diagram (Gibson *et al.* 2013).

NUCLEAR DESIGN

LANL was responsible for DUFF nuclear design. Neutronics calculations were performed with MCNP using the ENDF/B-7 cross section data (Poston *et al.* 2013). The results of the MCNP were very close to the experimental values. Table 9 shows main results of multiplication factor and reactivity for MCNP models and comparison with experimental data. The first Zero-Power Critical (ZPC) used a heat pipe with the same water loading as was used in the model. The experimental value was based on the measured excess reactivity of $0.50, which was indicated by the reactor period (calculated by the inhour equation). The second zero-power critical used the real DUFF heat pipe, which was fully filled with water (it was found to boost performance during test at GRC). Like shown in Table 9, the experimental value was obtained based on a measured excess reactivity of $0.67 (the extra water had added $0.17 of reactivity). All of the MCNP results had a statistical error of < 0.001%.

A very close comparison could be expected because every part of the Flattop assembly was modeled based on the original design drawings and ^{235}U is a widely studied isotope cross section. The stainless steel walls, nickel wick and water working fluid added absorption and moderation to the core and a complex mix of reflection and absorption in the reflection region. The worth of heat pipes was calculated as $0.18. The positive impact of reflection and moderation was mostly offset by parasitic absorption. Reactivity Temperature Coefficients (RTC) were calculated based on elevated temperature MCNP calculations, which were based on the material expansion correlations and the temperature dependent cross sections calculated by NJOY (McFarlane and Muir 1994). The system transient calculations used an additional RTC based on spreading of the reflector segments caused by core expansion. Reflector movements created thin gaps between the components, which were modeled by MCNP to investigate their impact on reactivity. In general, the RTCs were able to reproduce experimental data very well.

System dynamic modeling was made by FRINK (Poston *et al.* 2013), which uses simple point kinetics coupled with finite-difference thermal calculations. A set of differential equations was estimated by the Crank-Nicholson method and reduced with a matrix solver. Figure 35 shows a comparison between FRINK results and experimental data for the September 13th run, and Fig. 36 for the September 18th run.

Table 9. DUFF Neutronics data: expe-rimental and MCNP calculated.

Parameter	Experimental		Model
	1st ZPC	2nd ZPC	
k-eff	1.0034	1.0046	1.0029
Excess reactivity ($)	0.50	0.67	--
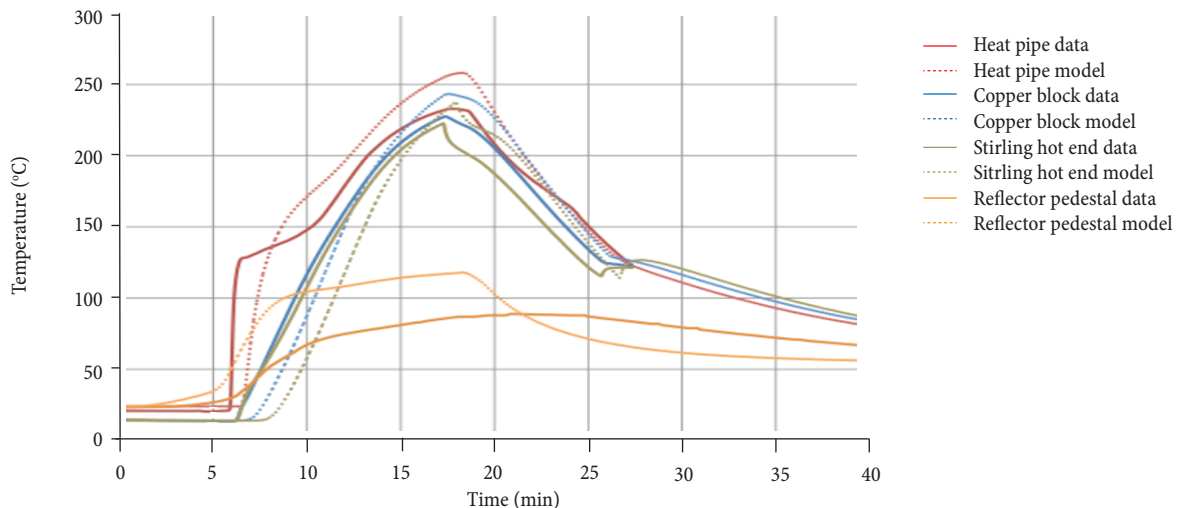
Figure 35. Experimental Data (continuous lines) and FRINK results (dashed lines) from September 13th run (Poston *et al.* 2013).
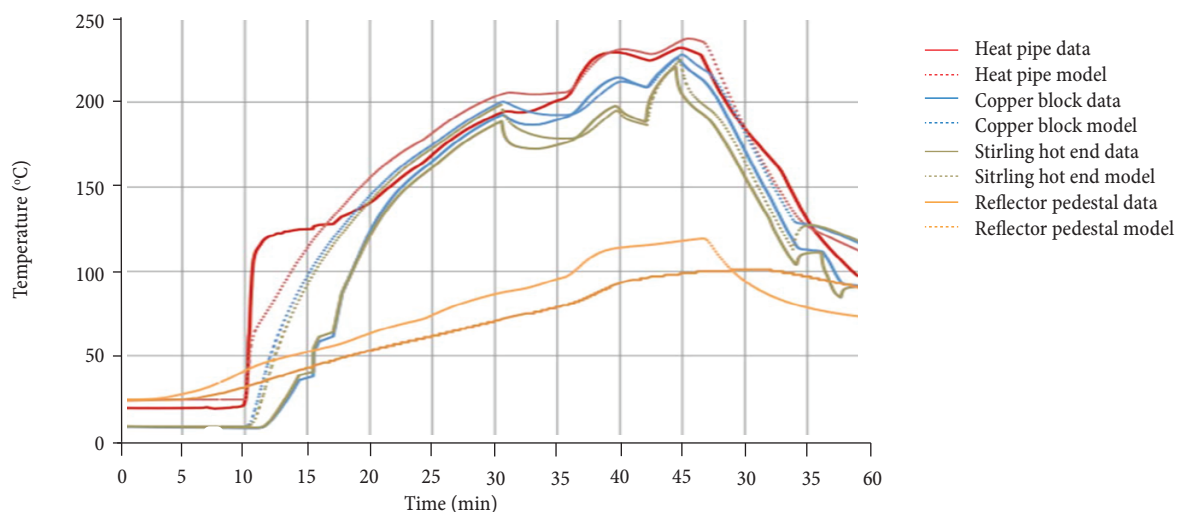
Figure 36. Experimental Data (continuous lines) and FRINK (dashed lines) results from September 18th run (Poston *et al.* 2013).

In both DUFF runs, the model was very accurate for the heat pipes and Stirling engines. FRINK solution did not match well with experimental data only in regions where temperatures were rapidly changing. The predicted peak temperature of the reflector did not match with reflector pedestal as well, but these were not the same locations. It is well known that point kinetics solution of neutron population is valid for compact, fast-spectrum reactors (Poston *et al.* 2013), and this was confirmed by FRINK calculations.

RESULTS

The two experiment runs accomplished the basic goal of illuminating a light panel with power from the Flattop. Figures 37 and 38 show the results for the two tests runs performed. In the first run, reactivity is quickly inserted and Stirling machines are turned on a few minutes later, producing a peak electrical output of ~24 We.
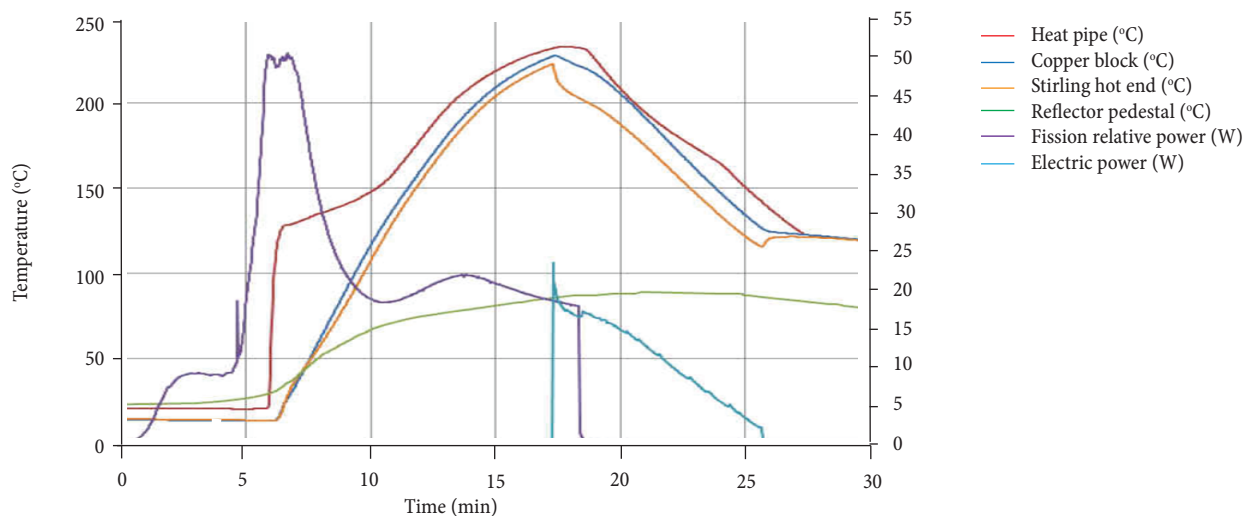
Figure 37. Data from DUFF September 13th run (Poston *et al.* 2013).
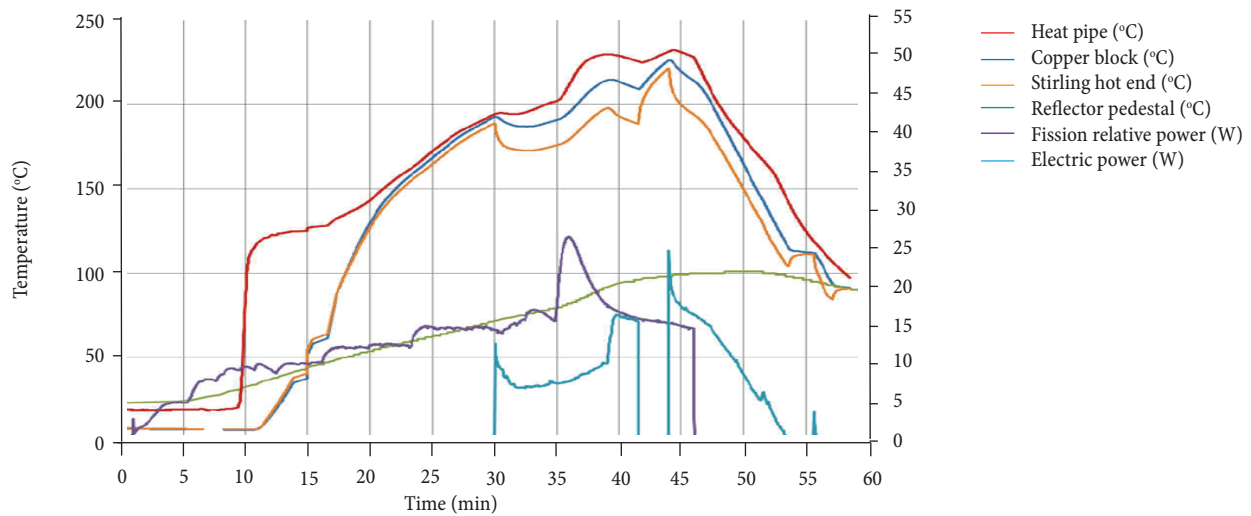
Figure 38. Data from DUFF September 18th run (Poston *et al.* 2013).

In the second run, reactivity is gradually increased, and the Stirling machines are first configured to operate in a lower power setting and then to a higher one, producing an increasing electrical output profile that reaches its maximum in ~24 We.

US SPACE NUCLEAR TECHNOLOGY: STATE OF THE ART

Although the TDU experiments have stopped, researchers have been working in technologies to be applied in Mars and Moon exploration. Tarau *et al.* (2016) report the development of the FSP heat pipe radiators, using a single facesheet radiator with heat pipes directly bonded it, which reduces mass and cost of the system, and Harris *et al.* (2017) investigate the thermodynamic behavior of a FSP system with Supercritical CO_2 Brayton Cycle instead of Stirling, using a heat transfer model to optimize system mass.

The Kilopower field is receiving a lot of attention mainly after the DUFF experiment. Hay and Anderson (2015) proposed and designed different water-titanium heat pipe configurations for Kilopower support. Rucker (2015) explores pros and cons of using small Kilopower fission systems instead of a large FSP for Mars missions.

NASA started testing a prototype Kilopower reactor by the end of 2017. The work follows on DUFF and is supported by the US National Nuclear Security Administration (NNSA). This prototype uses a solid ^{235}U core coupled to Stirling convertors by passive sodium heat pipes.

NASA GRC has managed all phases of the Kilopower project, with contributions from NASA MSFC. The NNSA's Y12 National Complex is providing the reactor core. NASA is partnering with the NNSS to carry out the tests, which will continue into early 2018. The prototype will undergo a fullpower test lasting for approximately 28 h (WNN 2017).

Alternative propulsion concepts with advanced technologies are being studied to improve systems performance. Some examples are Fission Fragment Engines and Pulsed Fission-Fusion. More detailed information is contained in Sudderth (2015).

CONCLUSIONS

This review presents a detailed description of the highlights of some of the fission power systems designed by US in the last four decades.

SPAR/SP-100 and SP-100 coupled nuclear fission to thermoelectric conversion, which was a well-known technology at the time and had shown to be safer and simpler due to the less number of components, reducing vibration and one-point-failure

chances. On the older hand, these systems were only able to achieve low thermal efficiencies, which required higher reactor size and output temperature. Prometheus and FSP strongly differed from then, not only in the reactor, but also in the power conversion concept, with the coupling of thermal cycles to the reactors in order to draw electricity. This allowed bigger payloads because of the efficiency increase.

The only described project that is currently in development is FSP, although tests with the TDU stopped due to PCU helium breach and the lack of funding to continue testing. DUFF was successfully completed and the other ones were shut down in the design phase, mostly for funding curtailment. These projects were more technologically aggressive, requiring higher amounts of budget and time. The DUFF experiment followed the reversed path, proving a complete nuclear concept in small scale, and saving money and time by using the existing structure, which lead to the project completion in less than a year with less than a million dollars.

DUFF marked a milestone in space nuclear technology, being the first system to produce electricity by using heat pipes to conduct heat from a nuclear reactor to Stirling convertors, and it is already being used as a basis for further development of fission power systems, mainly in the Kilopower field.

AUTHOR'S CONTRIBUTION

Conceptualization, Guimarães LNF; Methodology, Araújo EF; Investigation, Araújo EF and Guimarães LNF; Writing – Original Draft, Araújo EF; Writing – Review and Editing, Araújo EF and Guimarães LNF; Supervision, Guimarães LNF.

REFERENCES

Angelo Jr. J, Buden D (1985) Space nuclear power. Malabar: Robert E Krieger Pub. Co.

Araújo EF, Ribeiro GB, Guimarães LNF (2017) Regenerator optimization of a closed brayton cycle via entropy generation minimization. Presented at: International Nuclear Atlantic Conference; Belo Horizonte, Brazil.

Ashcroft J, Eshelman C (2007) Summary of NR program Prometheus efforts. Presented at: Space Technology and Applications International Forum. AIP Conference Proceedings; Maryland, USA. doi: 10.1063/1.2437490

Ashcroft J, Belanger S, Burdge W, Clementoni E, Jensen K, Proctor NB, Zemmo-Fulkerson A (2007) Key factors influencing the decisions on the number of Brayton units for the Prometheus space reactor. Presented at: Space Technology and Applications International Forum. AIP Conference Proceedings; Maryland, USA. doi: 10.1063/1.2437491

Borges EM, Sielaea JT (1992) Simulação e controle de escoamento do circuito primário de refrigeração do reator nuclear espacial SP-100. Presented at: 4th CGEN; Rio de Janeiro, Brazil.

Briggs MH, Gibson MA, Geng SM (2014) Status update for the fission surface power technology demonstration unit. Presented at: Nuclear and Emerging Technologies for Space; Albuquerque, USA.

Briggs MH, Gibson MA, Geng S, Sanzi J (2016) Fission surface power technology demonstration unit test results. Presented at: 14th International Energy Conversion Engineering Conference; Salt Lake City, USA. doi: 10.2514/6.2016-5012

Davison HW (1968) Compilation of thermophysical properties of liquid lithium. (TN-D-4650). NASA Technical Note.

Demuth SF (2003) SP 100 Space Reactor Design. Progress in nuclear energy 42(3):323-359. doi: 10.1016/S0149-1970(03)90003-5

Dixon D, McClure PR, Beller TE, Poston DI, Gibson MA, Bagg SD (2013) The DUFF experiment – why and how. Presented at: Nuclear and Emerging Technologies for Space; Albuquerque, USA.

El-Genk MS (2009) Deployment history and design considerations for space reactor power systems. Acta Astronautica 64(9-10):833-849. doi: 10.1016/j.actaastro.2008.12.016

El-Genk MS, Tournier JM (2008) Noble gas binary mixtures for gas-cooled reactor power plants. Nuclear Engineering and Design 238(6):1353-1372. doi: 10.1016/j.nucengdes.2007.10.021

[FSTP] Fission Surface Power Team (2010) Fission surface power initial concept definition. (TM-2010-216772). NASA Technical Report.

Gibson M, Briggs MH, Sanzi JL, Brace MH (2013) Heat pipe powered Stirling conversion for the Demonstration Using Flattop Fissions (DUFF) test. (TM-2013-216542). NASA Technical Report.

Guimarães LNF, Ribeiro GB, Nascimento JA, Araújo EF, Braz Filho FA, Dias AF, Leite VSFO, Placco GM (2017) TERRA: a nuclear reactor to help explore space, deep ocean and difficult access locations. Presented at: International Nuclear Atlantic Conference; Belo Horizonte, Brazil.

Harris KE, Schillo KJ, Hew YM, Kumar A, Howe SD (2017) Mass optimization of a supercritical CO2 Brayton cycle power conversion system for a mass surface fission power reactor. ASME J of Nuclear Rad Sci 3(3):031006. doi: 10.1115/1.4035974

Hay R, Anderson WG (2015) High Temperature Water-Titanium Heat Pipes for Spacecraft Fission Power. Presented at: Nuclear and Emerging Technologies for Space; Albuqueque, USA.

Koroteev AS, Oshev YA, Popov SA, Karevsky AV, Solodukhin AY, Zakharenkov LE, Semenkin AV (2015) Nuclear power propulsion system for spacecraft. Thermal Engineering 62(13):971-980. doi: 10.1134/S0040601515130078

Longhini EP, Lobo PDC, Guimarães LNF, Braz Filho FA, Ribeiro GB (2017) Brayton cycle numerical modeling using the RELAP5-3D code, version 4.3.4. Presented at: International Nuclear Atlantic Conference; Belo Horizonte, Brazil.

Lorentz DG (2007) Ex-Core CFD Analysis Results for the Prometheus Gas Reactor. Presented at: Space Technology and Applications International Forum; Albuquerque, USA.

MacFarlane R, Muir D (1994) The NJOY Nuclear Data Processing System Version 91. (LA-12740-M). LANL Technical Report.

Mason LS, Houts MG (2010) Fission Surface Power Technology Development Update. (TM-2011-216976). NASA Technical Report.

Mason L (2010) Recent advances in power conversion and heat rejection technology for fission surface power. Presented at: Nuclear and Emerging Technologies for Space 2009; Atlanta, USA.

Mason L, Gibson MA, Poston D (2013) Killowatt-class fission power systems for science and human precursor missions. (TM-2013-216541). NASA Technical Report.

McClure PR, Poston D (2013) Design and testing of small nuclear reactors for defense applications. Invited Talk to ANS Trinity Section; Santa Fe, USA.

Palac DT, Mason LS, Houts MG, Harlow S (2011) Fission surface power technology development update. (TM-2011-216976). NASA Technical Report.

Placco GM, Guimarães LNF, Santos GSB (2017) Design of a rankine cycle operating with a passive turbine multi fluid. Presented at: International Nuclear Atlantic Conference; Belo Horizonte, Brazil.

Poston DI, Kapernick RJ, Marcille TF, Sadasivan P, Dixon DD, Amiri BW (2006) Comparison of reactor technologies and designs for lunar/martian surface reactor applications. Presented at: International Congress on Advances in Nuclear Power Plants; Reno, USA.

Poston DI, Kapernick RJ, Dixon DD, Werner J, Qualls L, Radel R (2009) Reference reactor module design for NASA's lunar surface power system. Presented at: Nuclear and Emerging Technologies for Space; Atlanta, USA.

Poston DI, McClure PR, Dixon DD, Gibson MA (2013) The DUFF experiment – what was learned? Presented at: Nuclear and Emerging Technologies for Space; Albuquerque, USA.

Randall T (2005) Prometheus project final report. (982-R120461). NASA Technical Report.

Romano LFR, Ribeiro GB (2017) Optimal temperature of operation of the cold side of a closed Brayton cycle for space nuclear propulsion. Presented at: International Nuclear Atlantic Conference; Belo Horizonte, Brazil.

Rucker MA (2015) Integrated surface power strategy for Mars. Presented at: Nuclear and Emerging Technologies for Space; Albuquerque, USA.

Slewinski A, Caldeira AD, Ribeiro GB (2017) Generation of cross section data of heat pipe working fluids for compact nuclear reactors. Presented at: International Nuclear Atlantic Conference; Belo Horizonte, Brazil.

Smith JM (1989) SP-100 nuclear space power systems with application to space commercialization. Presented at: Space Commercialization: Roles of Developing Countries; Nashville, USA.

Sudderth LK (2015) A guide to nuclear technologies for space applications: past, present, and future. Presented at: Nuclear and Emerging Technologies for Space; Albuquerque, USA.

Tarau C, Maxwell TP, Anderson WG, Wagner C, Wrosch M, Briggs MH (2016) Status of the development of low cost radiator for surface fission power - II. Presented at: Nuclear and Emerging Technologies for Space; Huntsville, USA.

[WNN] World Nuclear News (2017) NASA to test prototype Kilopower reactor. World Nuclear News; [accessed 2018 January 3]. http://www.world-nuclear-news.org/ON-NASA-to-test-prototype-Kilopower-reactor-1711174.html